Annex 4
Summary of professional achievements

1. **First name and last name**

   Wojciech Milczarek

2. **Education, diplomas and scientific degrees awarded**

   - PhD in technical sciences in the mining and engineering geology discipline (specialty: engineering geodesy, protection of mining areas), Wroclaw University of Science and Technology, Faculty of Geoengineering, Mining and Geology, 2011.

   - Master's degree in engineering, geodesy and cartography, AGH University of Science and Technology, Faculty of Mining Surveying and Environmental Engineering, 2010.

   - Master's degree in engineering, mining and engineering geology, Wrocław University of Technology, Faculty of Geoengineering, Mining and Geology, 2006.

3. **Work experience in research institutions**

   - October 2013 - currently, Wrocław University of Science and Technology, Faculty of Geoengineering, Mining and Geology, Department of Geodesy and Geoinformatics, adjunct,

   - June 2012 - September 2012, University of New Brunswick, Canadian Center for Canadian Center for Geodetic Engineering, Fredericton, Canada, visiting researcher,

   - September 2011 - September 2013, Wroclaw University of Science and Technology, Faculty of Geoengineering, Mining and Geology, Department of Geodesy and Geoinformatics, research assistant.

   On October 1, 2011, I was employed as an assistant at the Department of Geodesy and Geoinformatics, Faculty of Geoengineering of Mining and Geology of the Wrocław University of Science and Technology. Two years later, I took the position of a research and didactic adjunct in the same institution. Continuously from 2012 I am the head of the postgraduate studies in *Geographical Information Systems* organized by the Center for Continuing Education and the Faculty of Geoengineering of Mining and Geology at the Wrocław University of Science and Technology. From 1 October 2016, I have been a vice-dean for Student Affairs at my home department.

   I presented foreign internships in Annex No. 5 (list of habilitation achievements), in item III (item L).

4. **Indication of the accomplishment arising from art. 16 sec. 2 of the Act of March 14, 2003 on Academic Degrees and Academic Title and on Art Degrees and Titles (Official Journal of Laws, No. 2016, Item 882, as amended)**

   A. **Subject of scientific achievement**

   This habilitation degree application is based on a set of seven thematically related articles published in journals listed in the Journal Citation Reports database and in one journal from the Ministry of Science and Higher Education List B. The academic achievement is titled:

   ## Application of Synthetic Aperture Radar Interferometry in the Identification of Ground Surface Displacements in Mining and Post-Mining Areas

   The series of publications presented below discusses particular issues related to the usage of synthetic aperture radar interferometry data in detecting displacements on the ground surface due to the influence of mining operations.

B. **List of thematically related publications constituting scientific accomplishment**

O1 **Milczarek W.**, Application of Small Baseline Subset Time Series Method with Atmospheric Correction in Monitoring Results of Mining Activity on Ground Surface and in Detecting Induced Seismic Events. Remote Sensing. 2019, (*article accepted for publication*).
IF = 3.406, **35 MoSaHE (MNiSW) points**

O2 **Milczarek W.**, Investigation of post inducted seismic deformation of the 2016 MW 4.2 Tarnovek Poland mining tremor based on DInSAR and SBAS method Acta Geodynamica et Geomaterialia. 2019, vol. 15, No. 2(194)
IF = 0.886, **20 MoSaHE (MNiSW) points**

O3 **Milczarek W.**, Kopec, A., Głąbicki D., Estimation of Tropospheric and Ionospheric Delay in DInSAR Calculations: Case Study of Areas Showing (Natural and Induced) Seismic Activity. Remote Sensing. 2019, 11, 621, doi: 10.3390/rs11060621
IF = 3.406, **35 MoSaHE (MNiSW) points**

My individual contribution is 80%.*

O4 Blachowski, J., Kopec, A., **Milczarek W.**, Owczarz, K. Evolution of Secondary Deformations Captured by Satellite Radar Interferometry: Case Study of an Abandoned Coal Basin in SW Poland. Sustainability 2019, 11, 884.
IF = 2.075, **20 MoSaHE (MNiSW) points**

My individual contribution is 70%.*

O5 Blachowski J., Jiránková E., Lazecký M., Kadlečík P., **Milczarek W.**, Application of satellite radar interferometry (PSInSAR) in analysis of secondary surface deformations in mining areas. Case studies from Czech Republic and Poland. Acta Geodynamica et Geomaterialia. 2018, vol. 15, nr 2, s. 173-185.
IF = 0.886, **20 MoSaHE (MNiSW) points**

O6 **Milczarek W**., Blachowski J., Grzempowski P., Application of PSInSAR for assessment of surface deformations in post-mining area - case study of the former Walbrzych hard coal basin (SW Poland). Acta Geodynamica et Geomaterialia. 2017, vol. 14, nr 1, s. 41-52.
IF = 0.886, **20 MoSaHE (MNiSW) points**

My individual contribution is 75%.*

O7 **Milczarek W**., Blachowski J., Grzempowski P., The use of satellite radar interferometry in surface deformation studies in brown coal mining. Opencast Mining. 2017, nr 1, s. 22-27 (in Polish).
IF = -, lista B, **7 MoSaHE (MNiSW) points**

My individual contribution is 75%.*

O8 Blachowski J., **Milczarek W**., Grzempowski P., Historical and present-day vertical movements on old mining terrains - case study of the Walbrzych coal basin (SW Poland). Acta Geodynamica et Geomaterialia. 2015, vol. 12, nr 3, s. 227-236.

IF = 0.561, 20 MoSaHE (MNiSW) points

My individual contribution is 25%.*

* - Statements of the authors of the publication (including the applicant) have been included in Annex No. 7.

C. **Discussion of the research objectives of the publications and achieved results together with discussion on their possible application**

Genesis of conducted research

My research activity and interests have always focused on describing the influence of mining exploitation on the ground surface. In the first years of my academic career, which were devoted to my doctoral dissertation, I concentrated on determining the extent of post-mining deformations, characteristic to areas in which mining activity ceased. The first research area was the Walbrzych region of hard coal mines (Walbrzyskie Kopalnie Wegla Kamiennego, further: WKWK). The purpose of the research works was to provide quantitative and qualitative data which allow accurate evaluation of the post-mining deformations of rock mass surfaces. The research works comprised inter alia:

+ development of a spatial geological model of the Walbrzych basin. The model was then integrated with the GIS-WKWK database, which contains spatial information among others on the range of mining operations performed since the beginning of the 19th century.
+ numerical calculations (finite element method), which were based on the author's original methodology for numerical calculations performed on both theoretical and actual models with allowance for mined seams and the restoration of groundwater table level in the rock mass. My calculations included the influence of local tectonic faults on the extent of ground surface displacements.
+ development and installation of a control-measurement network on a part of the WKWK region. The network consisted of GPS points, which were destabilized in the Walbrzych region and of level circuits. Between 2009 and 2010 the above network served me in two measurement campaigns.

Numerical calculations allowed me to demonstrate that the restoration of the Carboniferous water table level in the post-mining period had a significant influence on the uplift of the Walbrzych area. In some subareas of the former coal basin, the terrain surface lifted within the range of 5% to 8% of the vertical displacement values recorded during the functioning of the mining basin. Precise leveling which I performed between 2009 and 2010 in the measurement network, on a part of the old basin, revealed significant vertical displacements of the rock mass surface within the range of -14.1 mm do +3.5 mm. The results of simultaneous GPS measurements revealed significant horizontal rock mass surface displacements, within the range of 5-8 mm. Both vertical and horizontal displacements prove that the rock mass surface in the area is still active.

The above details of my doctoral research program have been here provided in order to clearly distinguish between my research before and after obtaining the doctoral degree.

After obtaining the doctoral degree, I gradually shifted my research interests towards the broadly understood synthetic aperture radar interferometry. The experience I had gained during my PhD studies convinced me that in the near future InSAR methods may become an alternative to classical measurements (precise leveling, GNSS) of mining and post-mining ground surface deformations.

Introduction

Synthetic aperture radar interferometry is one of the remote techniques used in Earth surface observations. It allows detecting surface displacements due to natural geological phenomena, as well as tectonic, volcanic and anthropogenic processes. Spatially, InSAR allows detecting ground surface changes of various scale: from minor local events such as mining tremors to larger, regional

events such as earthquakes. The InSAR method dates back to 1978, when the first satellite equipped with SAR instruments, named SEASAT-1 (NASA), was put on the orbit of the Earth. However, InSAR methods were most intensively developed in the 1990s. During this decade, national and international space agencies sent the following satellites to the orbit: ERS-1 (1991), JERS-1 (1992), ERS-2 (1995), RADARSAT-1 (1995). More satellites were placed on the orbit in the following years (Fig. 1).

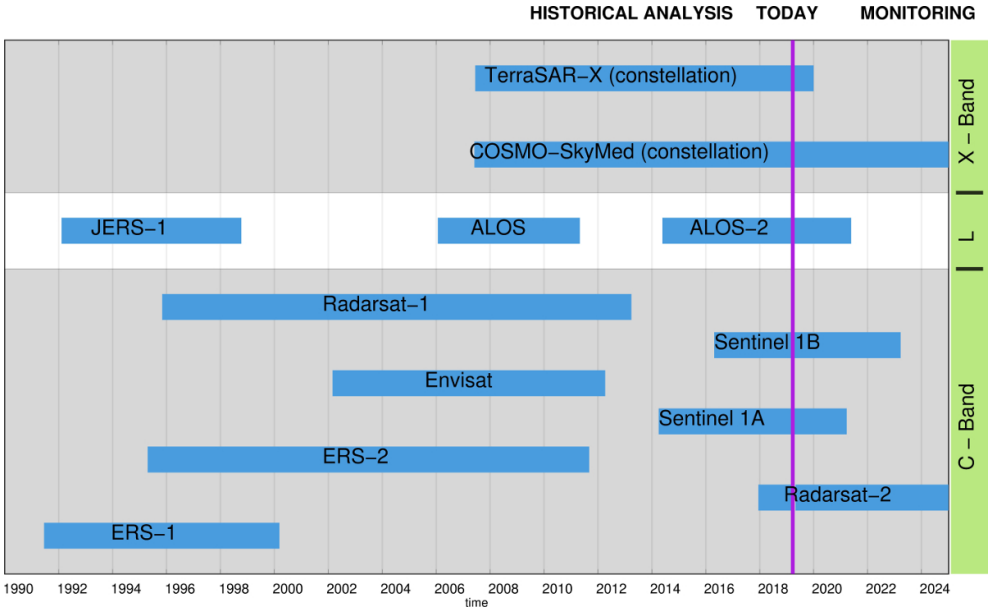

Fig. 1: Selected satellites equipped with SAR apparatus used in surface monitoring.

The SAR data, which have been collected for more than 25 years, allow the analysis of historical events. The currently active satellites, among others Sentiel 1A, Sentinel 1B, TerraSAR-X (constellation of satellites), Cosmo-SkyMed (constellation of satellites), or ALOS-2, allow continuous monitoring of the surface of any area on the planet.

The basic result of the processing of two radar images is the interferogram, which in addition to information about the deformation of the terrain surface also contains a number of other components. A general equation of the interferometric phase $\Delta\varphi$ calculated from two SAR acquisitions may be shown as follows:

$$\Delta\varphi = \frac{4\pi}{\lambda}(\Delta r^{ij}_{disp} + \Delta r^{ij}_{geom} + \Delta r^{ij}_{trop} + \Delta r^{ij}_{iono} + \Delta r^{ij}_{n}) \tag{1}$$

where: λ represents the carrier wavelength of the radar, Δr^{ij}_{disp} is the ground displacement in radar LOS direction, Δr^{ij}_{geom} represents the geometrical range difference from radar to the target caused by a nonzero spatial baseline between the two orbits, Δr^{ij}_{trop} is tropospheric delay, Δr^{ij}_{iono} is ionospheric delay, and Δr^{ij}_{n} it is thermal noise and variability of scattering.
The deformation component contains information on possible displacements between subsequent radar data acquisition. Designation Δr^{ij}_{disp} is crucial in calculations using InSAR methods.Nevertheless, often the sum of the other components is so significant that it makes it difficult or even impossible to determine the displacements sought. With the current state of knowledge, topographic components and orbital errors can be determined in a relatively easy way. However, the atmospheric delay, which consists of the ionosphere and tropospheric influences in relation to InSAR methods, is currently the subject of intensive research (Li et al., 2009; Doin et al., 2009; Brcic et al., 2010; Rosen et al., 2010; Bekaert et al., 2015; Gomba et al., 2016; Fattahi et al., 2017; Yu et al., 2018; Zhu et al., 2018).

Ground surface deformations due to underground mining activity belong to the most important negative results of human intervention in the rock mass. Depending on the geological conditions, they may have a continuous or non-continuous character. The methods most frequently used to measure ground surface deformations in mining areas include: precise leveling lines and GNSS measurements. The above list of methods should be also supplemented with methods based on synthetic

aperture radar interferometry and ground-based InSAR (Antonello et al., 2004; Carlà et al., 2018). The currently used InSAR methods include the differential method (Duque et al., 2007; Paradella et al., 2015; Peduto et al., 2017) and the time-series methods: PSInSAR and its variations (Jung et al., 2007; Liu et al., 2014), as well as SBAS (Ma et al., 2016; Zhao et al., 2013). InSAR methods are also successfully employed in detecting ground surface deformations in post-mining areas, i.e. the so-called post-mining deformations (Samsonov et al., 2013; Cuenca et al., 2013; Blachowski et al., 2019). In some cases, underground mining operations may lead to induced seismic events. The impact of induced seismic, as well as the impact of underground mining on surfaces, can also be observed using satellite radar data (Malinowska et al., 2018; Milczarek, 2019).

Scientific objective

The publication series (under a common title: *Application of Synthetic Aperture Radar Interferometry in the Identification of Ground Surface Displacements in Mining and Post-Mining Areas*) here discussed concentrated on a single problem of the possibility to use synthetic aperture radar interferometry in mining and post-mining areas. This general research goal required me to formulate the following particular research goals:

I to demonstrate the possibility of applying the time-series type InSAR methods (PSInSAR and SBAS) to investigate long-term surface displacements in mining and post-mining areas,

II to develop a method for simultaneous estimation of the influence of tropospheric and ionospheric delay on the calculated SAR data,

III to demonstrate the possibility of applying InSAR methods in the detection of induced seismic events in mining areas.

The above particular research goals are strictly related and their order is of significance. My first attempts at using SAR data were related to the Walbrzych region. The oldest publication in this series (**O8**) presents the results of the analysis of ground surface displacements in the Walbrzych post-mining area. My analyses were based on land survey data representing the national geodetic survey of second class as measured in 1973 and 1993. I also used the results of geodetic measurements performed in 2014 with the help of a geodetic network I designed as part of a research project titled: *Determining Ground Surface Activity in the Post-Exploitation Area of the Walbrzych Hard Coal Mines*, which I supervised. The analysis involved various interpolation functions and calculations based on map algebra and allowed inter alia defining ground surface displacements during final years of exploitation (1990s) and after mining activity ceased. Nevertheless, this publication marks the beginning of my research works related to the use of InSAR methods in the monitoring of surface activity in mining and post-mining areas. The fundamental weakness of the resultant data presented in (**O8**) consisted in their time- and space-arrangement. This was firstly due to the difficulties related to the analysis of secondary deformations, which have relatively limited – and, importantly, further declining – annual dynamics. The second obstacle was the size of the analyzed set which served to calculate surface displacements in the Walbrzych area. On the hand, the displacements observed on the bench-marks for the period of 1993-2014 point to an unfinished process of rock mass stabilization in the post-mining period and a delayed reaction of the rock mass to the reconstruction of the water table returning to original level after mining activity ceased. This fact indicates that post-mining deformations can be still observed and investigated in the area of Walbrzych. However, at that period no data existed which could serve to describe the process.

At this stage of my research, I was drawn to synthetic aperture radar interferometry. Literature studies demonstrated that some publications already existed, which discussed calculating displacements in post-mining areas in Europe (Samsonov et al., 2013; Cuenca et al., 2013). The major discrepancy between the discussed areas in Europe and the Walbrzych region resulted from the availability of different measurement data (precise leveling, GNSS). For this reason, the Walbrzych region has still remained unique to some extent, as research areas of such characteristics are difficult to find. The reason behind this phenomenon is that all of the WKWK mines were closed almost simultaneously. During this process, the drainage of rock mass was gradually stopped and the workings were flooded after the underground water was no longer pumped. Using natural hydrogeological conditions, the rock mass was divided into separate reservoirs, which were flooded independently. At the same time, no cyclical geodetic surveys were conducted which could provide data on the surface activity over that period.

During that period, application of synthetic aperture radar interferometry seemed to be the natural direction for further research. Theoretically, InSAR methods allow the analysis of historic data (starting in 1995, Fig. 1) as well as continuous and almost real-time monitoring of an area.

The possibility of applying the time-series type InSAR methods (PSInSAR and SBAS) to investigate long-term surface displacements in mining and post-mining areas

A number of research centers both in Poland and abroad focus on the problem of identifying the influence of underground mining on the rock mass surfaces. This extensive interest results from the fact that the processes which occur in the mined rock mass are very complicated to demonstrate and difficult to describe. The majority of the methods currently used to evaluate how mining activity influences the surface, also the methods aimed at forecasting this influence, at some point require information on actual surface displacements to be provided. In such case, the data are obtained from precise leveling or with the use of broadly understood GNSS measurements.

Secondary deformations, frequently also referred to as post-mining deformations, are characteristic of areas in which mining activity was finished. This type of deformations is related to the processes which occur inside the rock mass, mainly due to the reconstruction of water table levels. As a result, vertical displacements of ground surface observed over that period may have reverse direction (uplift) in comparison to displacements observed during mining activity (subsidence).

Walbrzych region

Publication (**O6**) demonstrated the first results of using SAR data in the area of Walbrzych. I based my calculations on the data obtained from the Envisat satellite for the period between 2002 and 2009. The total number of images was 21. The radar images were processed with the use of the persistent scatterers method (PSInSAR). The choice of a proper image, the so-called master image (Fig. 2), remains of key importance in this method. Master image serves to determine pairs of SAR images, and subsequently – interferograms. The calculations produced a set of points (approximately 10 000) for which Line-of-Sight (LOS) displacements were identified. The majority of points were located within the city border, as most of the persistent scatterers, i.e. building roofs or surfaces of other building structures are located in urban areas. Mean point density was about 30 per km^2. The analysis of the distribution of PS points with significant positive movement (more than 1 mm/year) showed that their majority was located within the boundaries of former mining areas in Walbrzych. Significant movements upwards (i.e. uplifts) were observed in the central and in southern parts of the former mining areas (Fig. 4).. The largest group are PS points with average

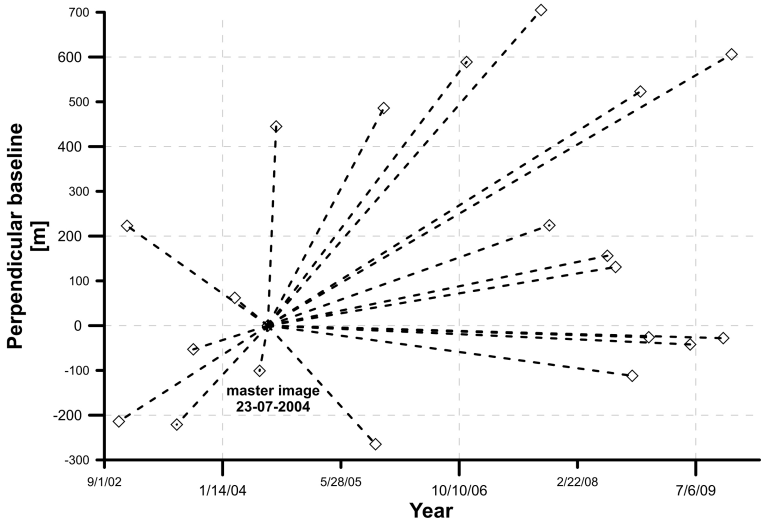

Fig. 2: Baseline information for the ENVISAT ASAR. The centre of the connecting lines is the master scene for the ENVISAT ASAR dataset. The image of 23-07-2004 was selected as the master image (**O6**).

annual movements in the range from -1.0 mm to + 1.0 mm (marked in gray) (Fig. 4). Publication

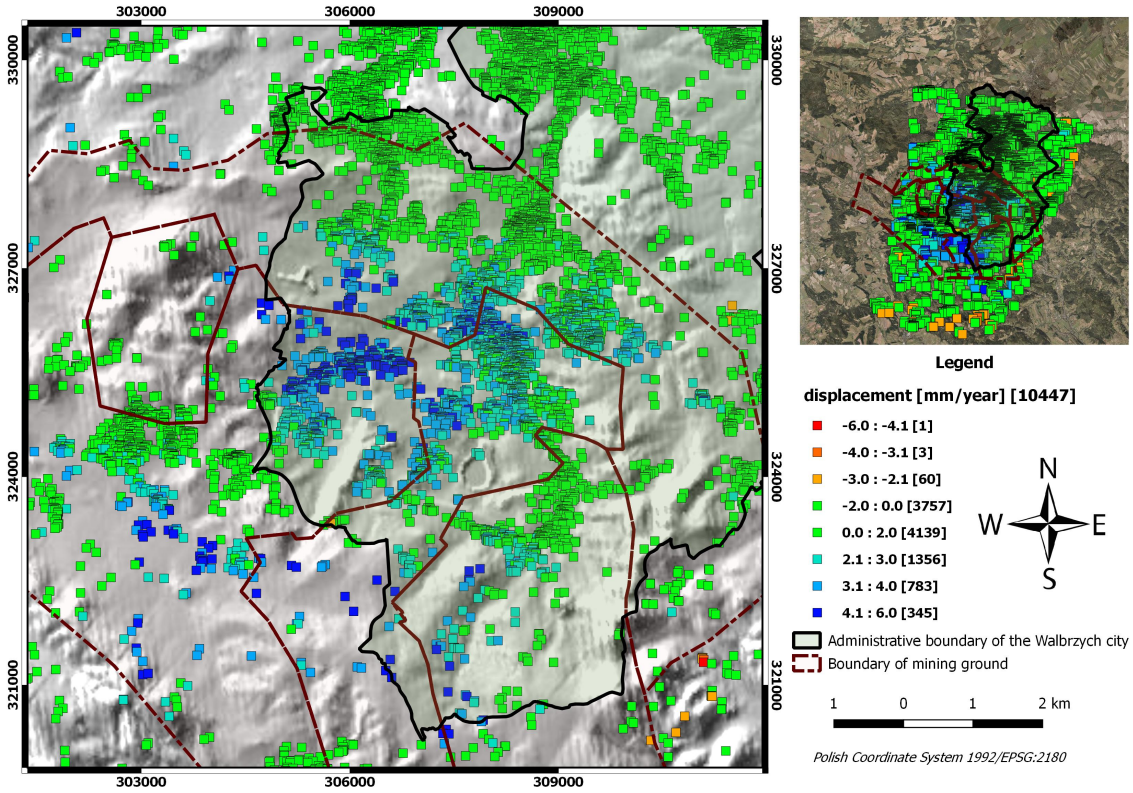

Fig. 3: Spatial distribution of PS points and boundaries of former mining areas in Wałbrzych (**O6**).

(**O6**) is the first item in the country that concerns analysis of displacements during the after-mining activity period using the InSAR methods in relation to the entire inactive basin.

Continued research in the region of Walbrzych resulted in two more publications (**O5**) and (**O4**).

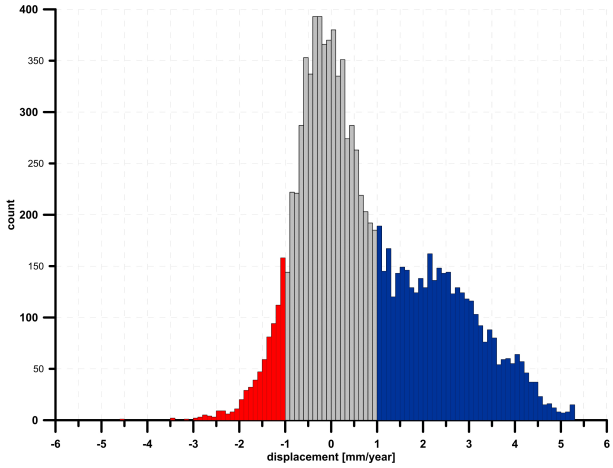

Fig. 4: Empirical distribution of average annual movements of PS points (in Line of Sight). Blue represents upward movement, red represents subsidence and grey represents points with movement values within the accuracy limits (**O6**).

Publication (**O5**) was prepared in cooperation with researchers from the Faculty of Mining and Geology, VSB-TU Ostrava. Calculations were performed on the basis of the PSInSAR method and the results were analyzed with respect to two regions: the Walbrzych region and the Ostrava-Karviná region in Czech Republic. Unlike in publication (**O6**), in this case I used (for the Walbrzych region) SAR data obtained from the ERS-1 and ERS-2 satellites for the period of 1995-2000. Additionally, I performed calculations for the independent tracks (79 and 308).

The obtained results are particularly interesting, as areas were identified in which local displacements over the analyzed period had a completely different character (Fig. 5). PPreliminary analysis of the results and comparison with the location of underground water reservoirs provided grounds for a thesis that local displacements may be linked to the process of restoring hydrogeological conditions in the period after mining activity is finished. Therefore, I decided to continue research in this area. The results were published in the next article (**O4**).

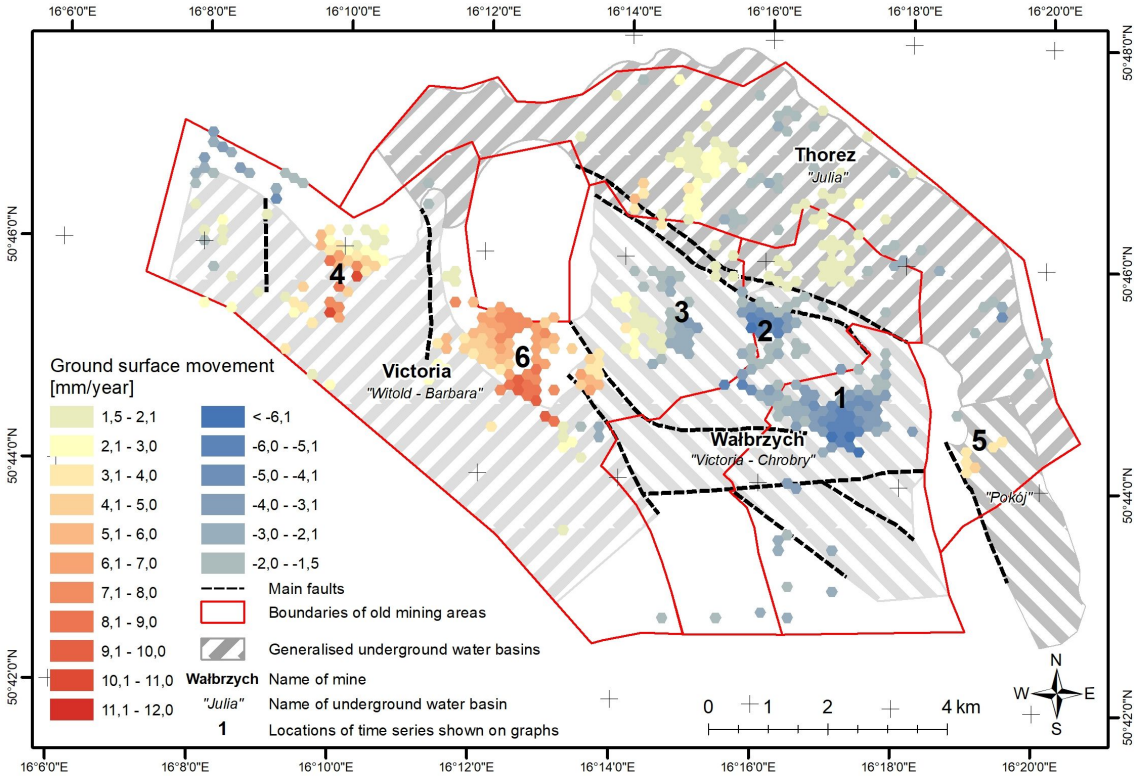

Fig. 5: Average movements (LOS) of ground surface between 1995-2000 in the Wałbrzych Coal Basin (**O5**)

The third article (**O4**) on ground surface displacements in the area of Walbrzych is the last publication and in a sense a summary of several years of research conducted in this region. The article is important for the following reasons. Firstly, it presents calculations for the complete period of 1995-2010, for which the analysis was possible. Secondly, the results were correlated with the water table levels obtained from the piezometers available in the area of Walbrzych. Thirdly, when selecting the master image from the ERS dataset, it was necessary to solve a problem resulting from significant divergence of the perpendicular baseline (Fig. 6) and from the high difference in the Doppler centroid values (which often exceed 2000 Hz). I did not perform the analysis of data from 1992, because SAR data from the beginning of 1993 until the end of 1994 was recorded in extremely different positions (Fig. 7). However, despite many attempts to select the proper master image, it was impossible to obtain reliable results for the 2002-2010 period. For this reason, I based the analysis for the period after 2002 on Envisat images, which have much more advantageous values of the perpendicular baseline and the difference in the Doppler centroid parameters for potential pairs.

Fourthly, the LOS results from the ERS-1/2 and Envisat satellites were transformed into one system. This approach made it possible to analyze the surface activity from 1995 to 2010. I conducted a thorough analysis of the breakdown in the process of liquidation of the extracted groundwater reservoirs (Fig. 8).

Summary

In the first period (1995-2000), two active areas are clearly visible on the surface. The first area was located within the borders of the "Witold-Barbara" reservoir and showed uplift with a ma-

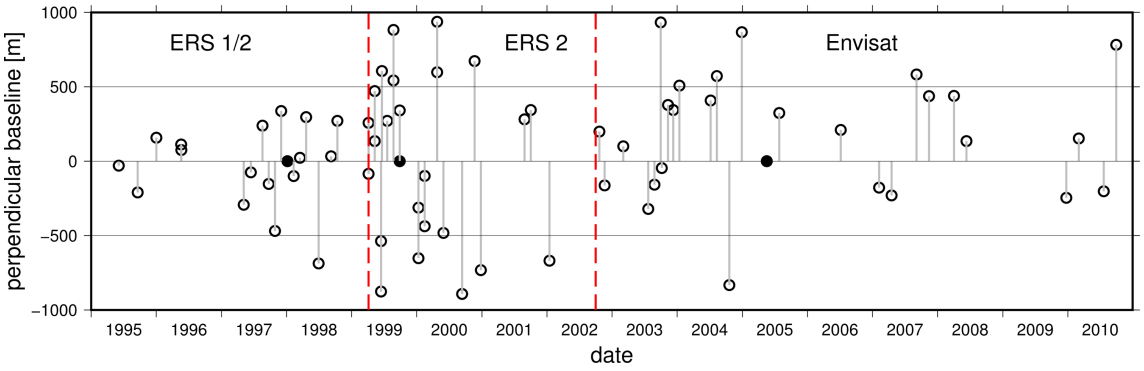

Fig. 6: List of the SAR data used: ERS from 1995–2000, ERS from 1999–2003, and Envisat from 2002–2010. Black dots represent master images for each of the calculation sets. Vertical dashed lines represent the borders between the sets (**O4**).

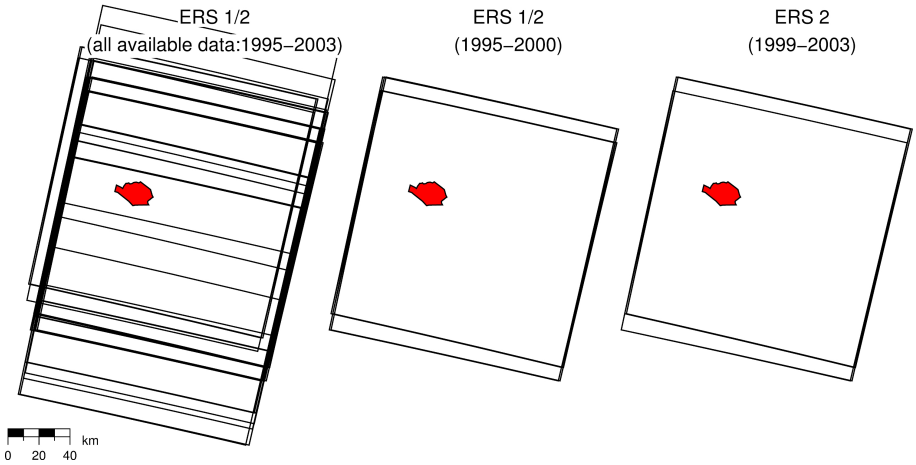

Fig. 7: Selection of SAR data from ERS 1/2. The red polygon corresponds to the borders of the WHCB mining areas. The left-hand side of the figure shows the spatial distribution of SAR data from the analyzed Path 308, for the 1995–2010 period, a total of 147 images. It is interesting to observe the scale of image shift in the E-W direction, which is maximally 11 km. The middle part of the figure shows selected images for the 1995–2000 period and the right-hand side for the 1999–2002 period (**04**).

ximum speed of +6 mm/year. During this period, the reservoir was subjected to flooding (1995 - 1999). The ground surface over the southern part of the "Victoria-Chrobry" reservoir subsided with a maximum speed of -6 mm/year. During this period, the analyzed area was subjected to mining activity. Observations during the second period (1999 - 2002) clearly show restoration of the underground water level in the "Julia" reservoir. As a result, uplift recorded on the surface reaches up to +8 mm/year. In the 2002 - 2010 period, uplift is observed in the central part of the basin. This phenomenon is likely due to the combined effect of the restored water table levels in the „Victoria-Chrobry" and „Julia" reservoirs. The results obtained for the WKWK region are similar to the results obtained for the Limburg region (Germany) (Cuenca et al., 2013). This similarity covers not only the recorded scale of upward movements (above 20 cm over 18 years), but also the dynamic characteristics of the phenomenon. The presented results, as is the case in the WKWK region, clearly indicate a direct correlation between rising underground water levels and upward movements of post-mining grounds. A similar ground surface movement was observed in Northumberland (Gee et al., 2017). In some cases (e.g. the Westoe region) the results of ground movements calculated from ERS 1/2 did not correlate with hydrogeological data. An interesting observation comes from (Samsonov et al., 2013), who noticed that in the case of the observed uplifts in the post-mining areas of the French-German border region, the movements were not always located directly over the flooded workings. This fact is due to the geological and tectonic structure and to the spatial arrangement of roadways and workings. With this observation applied to the conditions of the WCF area, I concluded that specific geological structure and local tectonic faults caused the influence of the flooded reservoir to be always observed directly over the reservoir.

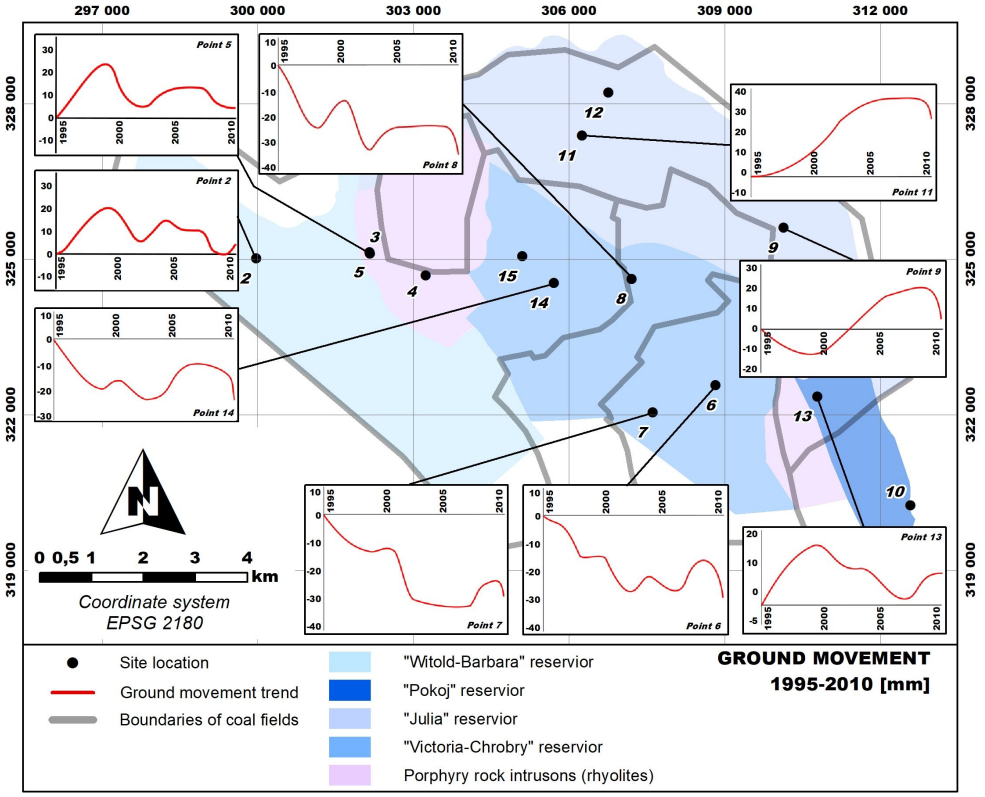

Fig. 8: Location of the representative points, which served to plot LOS ground movement graphs between 1995 and 2010 (**O4**).

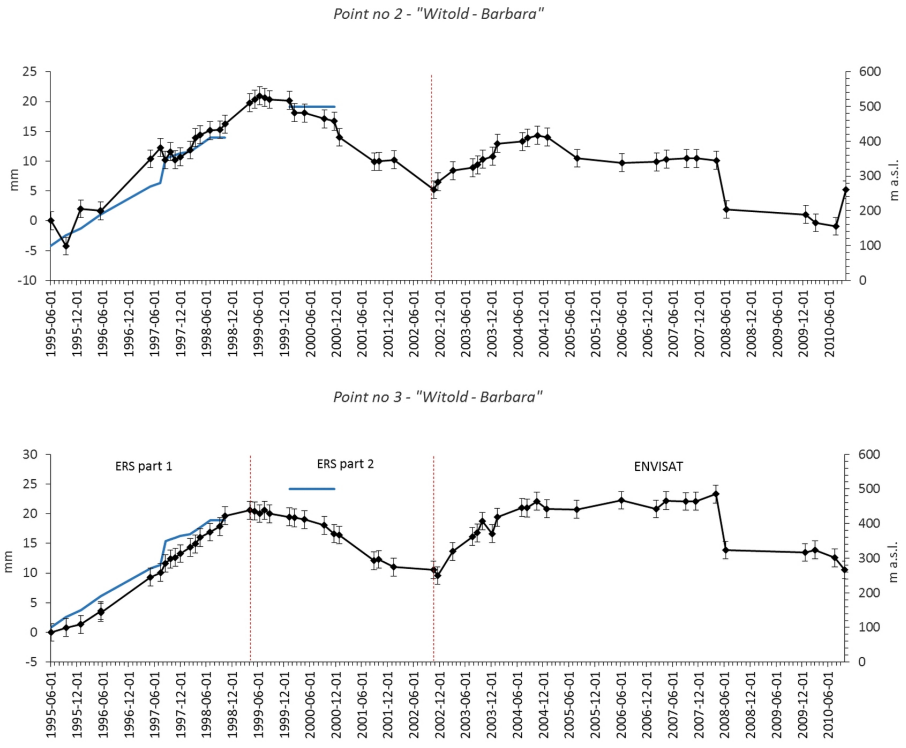

Fig. 9: Graphs of LOS displacements for Points 2, 3, 4, and 5 located in the Witold-Barbara reservoir area (**O4**).

To sum up, ground movements observed from SAR data calculations and presented in publications (**O4**, **O5**, **O6** and **O8**) showed local uplifts, which have been found to demonstrate clear

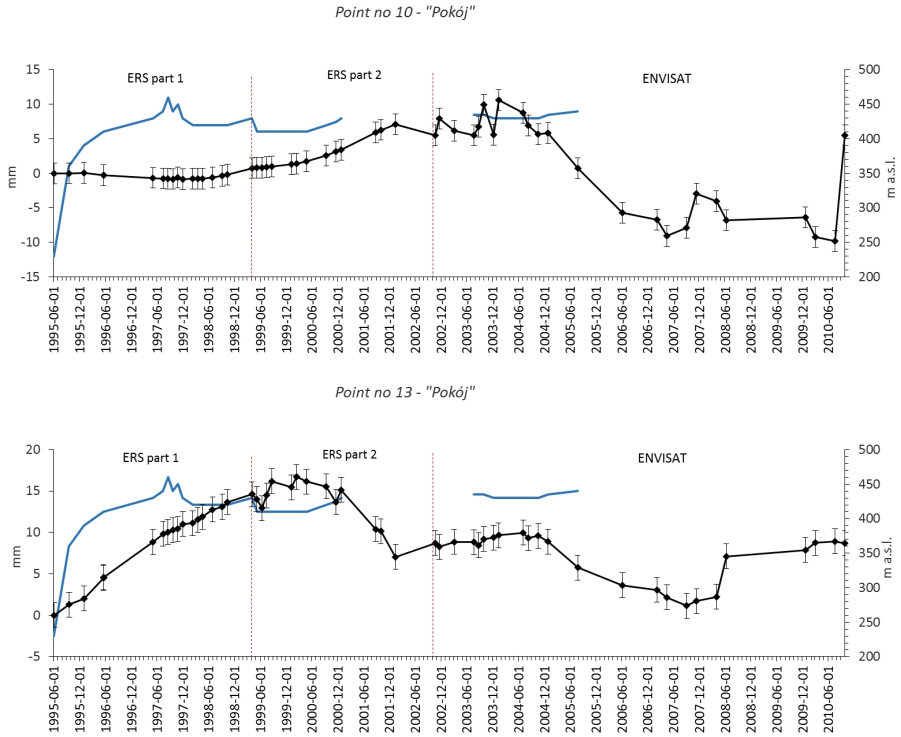

Fig. 10: Graphs of LOS displacements for Points 9, 11, and 12 located over the Pokoj reservoir (**O4**).

relationship between flooding of underground water reservoirs and ground upward movements. The conclusions I reached are similar to examples from literature. I also observed that controlled flooding of post-mining workings carried out over a long period of time minimized the effects of the process on the ground surface. The analyses in this paper prove that the period of ground upward movement, directly related to the restoration of groundwater table level, is followed by a short period of stagnation and then by a sort of ground movement adjustment. This adjustment is characterized by ground subsidence and followed by eventual surface stabilization (Fig. 9 - 10).

Turow brown coal mine

After conducting research in the Walbrzych region, I focused my attention on evaluating the possibility to use interferometric data for areas with ongoing mining activity. Publication (**O7**) from this series investigates the application of data from the Sentinel 1A satellite in the area of an open cast mine. The work related to the Turow brown coal mine is the first study of this type, in which ground surface activity was estimated in an open cast mine in Poland (including the pit, the dumping ground and the adjacent area). Based on my literature studies, I may conclude that this work is also one of the first in the world in which the SBAS method was employed and combined with data obtained from the Sentinel 1A/B satellite.

Based on calculations performed for one year (Nov. 2015 – Nov. 2016), (**O7**) demonstrates that radar interferometry may be used to monitor an area and detect potential displacements. The calculated maximum subsidence in the inner dumping ground reached 43 cm/year (Fig. 11). Additionally, I managed to identify the area of the slope in the eastern part of the mine pit, where subsidence was observed. This area had not yet been subjected to any works comprising removal of the overburden, mineral exploitation or dumping of waste, and the observed displacements indicate that it slowly subsides..

The obtained results provided another piece of important information. Figure 12 shows the increments of displacements determined from subsequent SAR data on the profile through the area of the pit. In this case, mean interval between successive data acquisitions was 12 days. The curves in the graph, which represent displacement increments, intersect in many locations. Additionally,

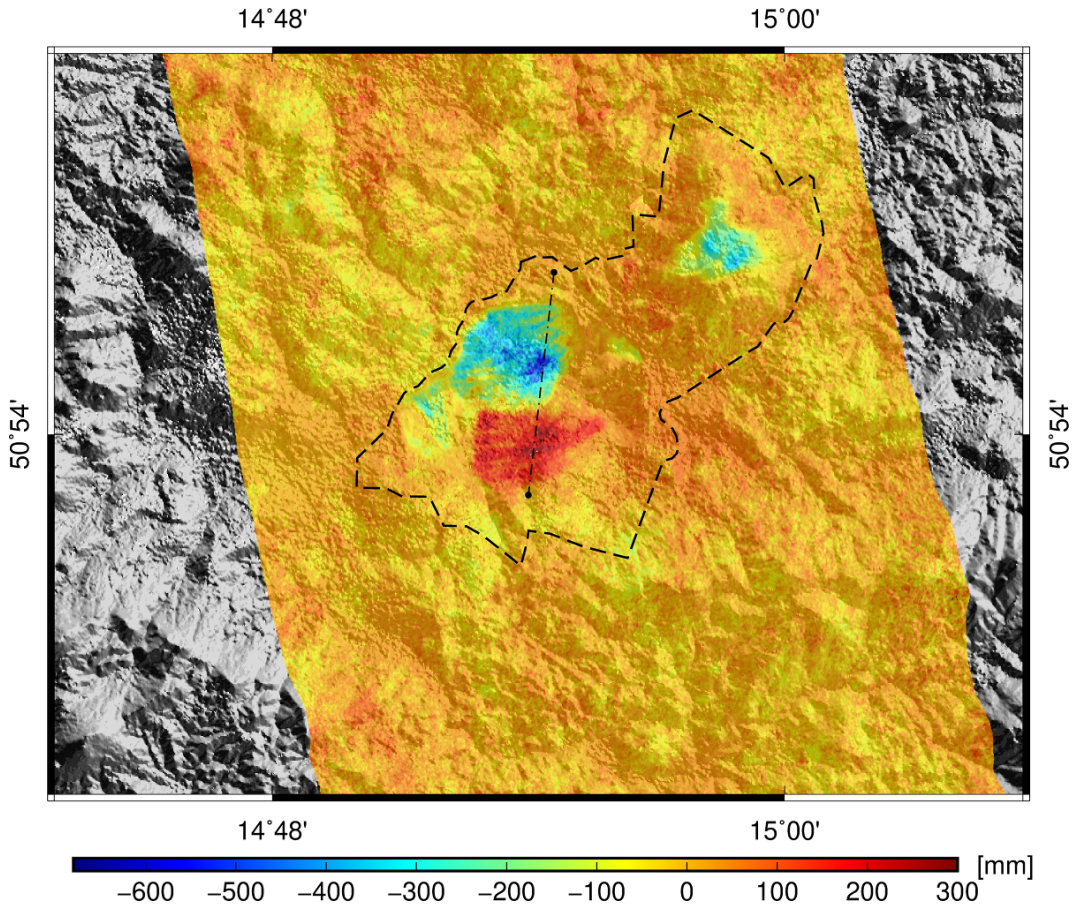

Fig. 11: LOS displacements during 22/11/2015 - 11/04/2016 SBAS designated by black dashed lines indicate the profile of displacement of the selected portion of the mining area (**O7**).

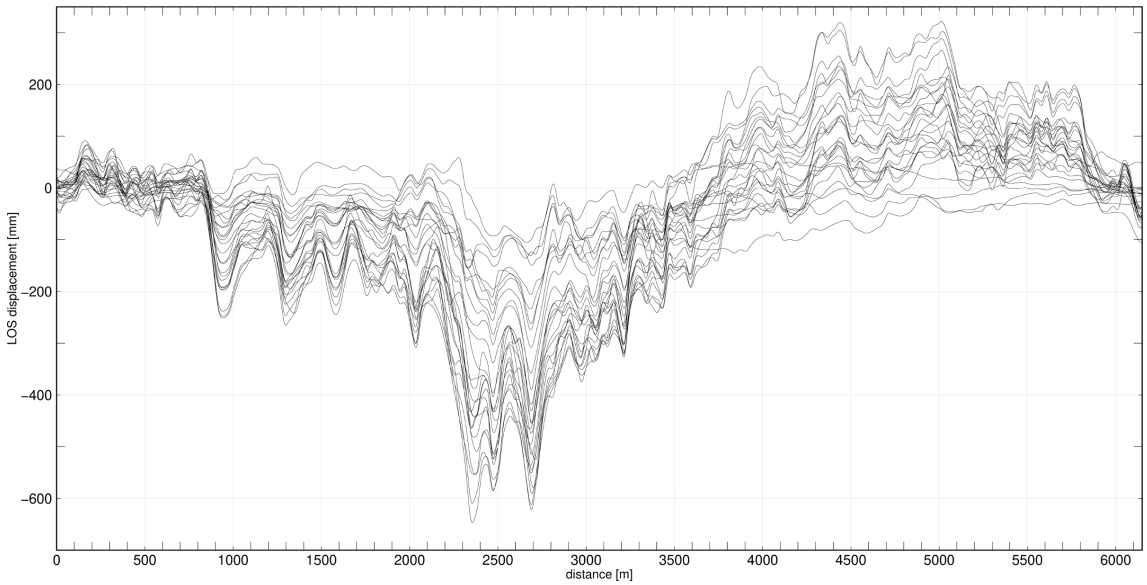

Fig. 12: LOS displacement increments determined for the profile marked in Fig. 11, the average interval between consecutive results was 12 days.

their patterns are occasionally illogical. My experience at that time allowed me to expect that this phenomenon is caused by the fact that the signal passes through the atmosphere. This may significantly affect the final results. Comparing displacements in much larger time intervals (Fig. 13) may be noted that the displacement increases are to each other they are much more consistent

than in the case of interval 12 days. I argue that this fact demonstrates the negative influence of atmospheric delays.

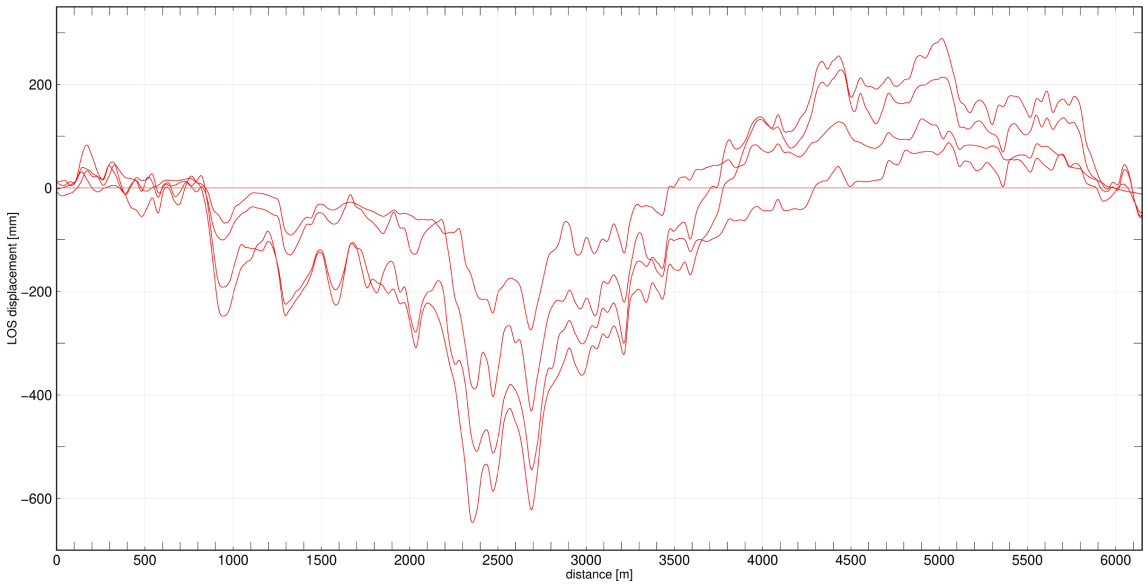

Fig. 13: LOS displacement increments determined for the profile indicated in Fig. 11, the average interval between consecutive results was about 3 months.

Legnica-Glogow Copper Belt - LGCB

The Legnica-Glogow Copper Belt (LGCB) was the next mining area which served me to calculate ground surface displacements on the basis of SAR data from satellites Sentinel 1A/B. As in the case of the Turow brown coal mine, the SBAS method was also used to analyze the influence of underground mining activity on ground surface in the LGCB region. The obtained results and their analysis was presented in (**O3**). Unlike in the case of the Turow brown coal mine, I performed calculations for two independent sets obtained from two tracks: 22 and 79 (Tab. 1). The time scope and the number of interferograms obtained from SBAS calculations were also important. The analyzed period covered the whole currently available time range, i.e. from November 2014 until May 2018. My calculations included all available radar data acquisitions. Therefore, I was able to analyze displacements with the shortest possible time interval of six days

Tab. 1: Scene acquisition basic information (**O1**).

path	**22**	**73**
satellites	Sentinel 1A/1B	Sentinel 1A/1B
number of SAR data acquired	123	122
time range	06/12/2014 ÷ 19/05/2018	15/11/2014 ÷ 15/05/2018
number of interferograms	420	436

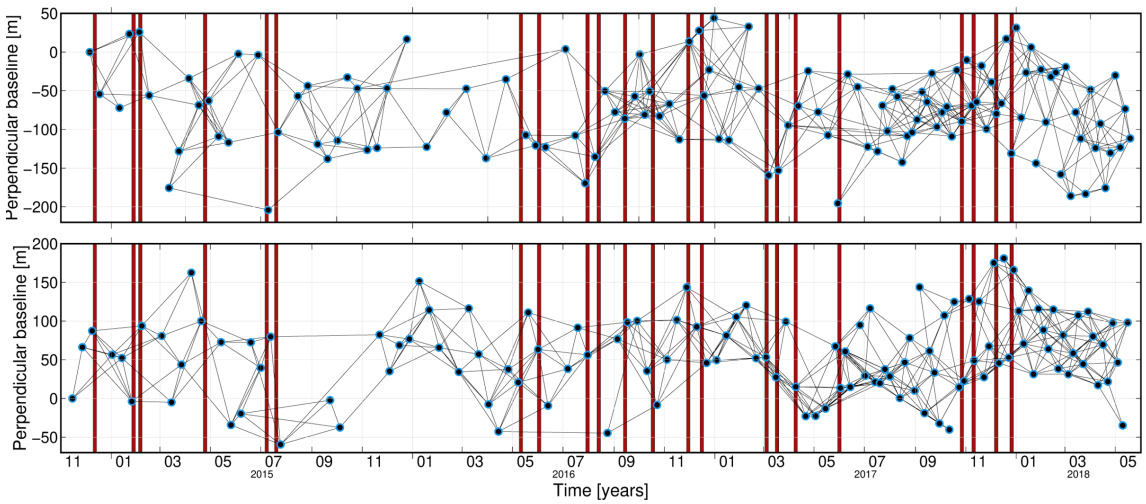

Fig. 14: Baseline plot for the two SAR data sets obtained from path 22 (above) and path 73 (below). The analyzed period spanned the years from 2014 to 2018. Red vertical lines denote recorded induced seismic events exceeding magnitude Mw 3.9 (**01**).

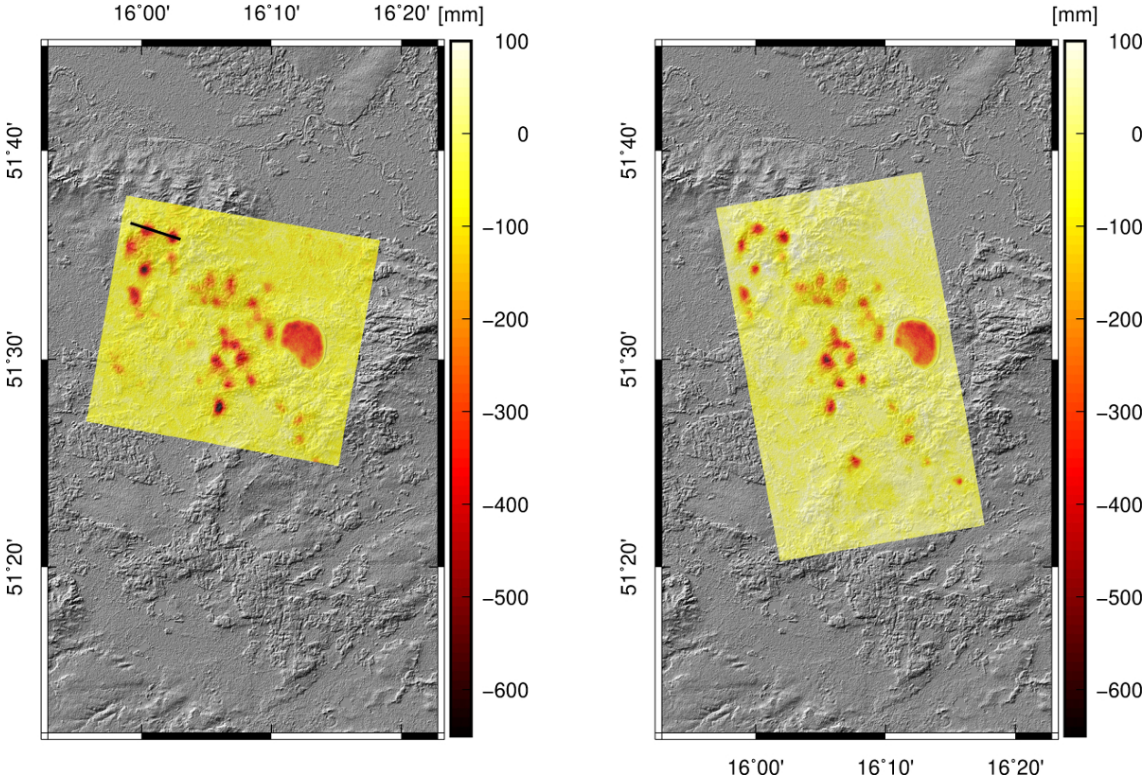

Fig. 15: The results of LOS displacement calculations for the LGCB area from two paths 22 (right) and 73 (left). The figure presents total LOS displacements for the analyzed period, the black line on the left map represents the course of the profile for which the displacement graph was drawn (Fig. 16) (**01**).

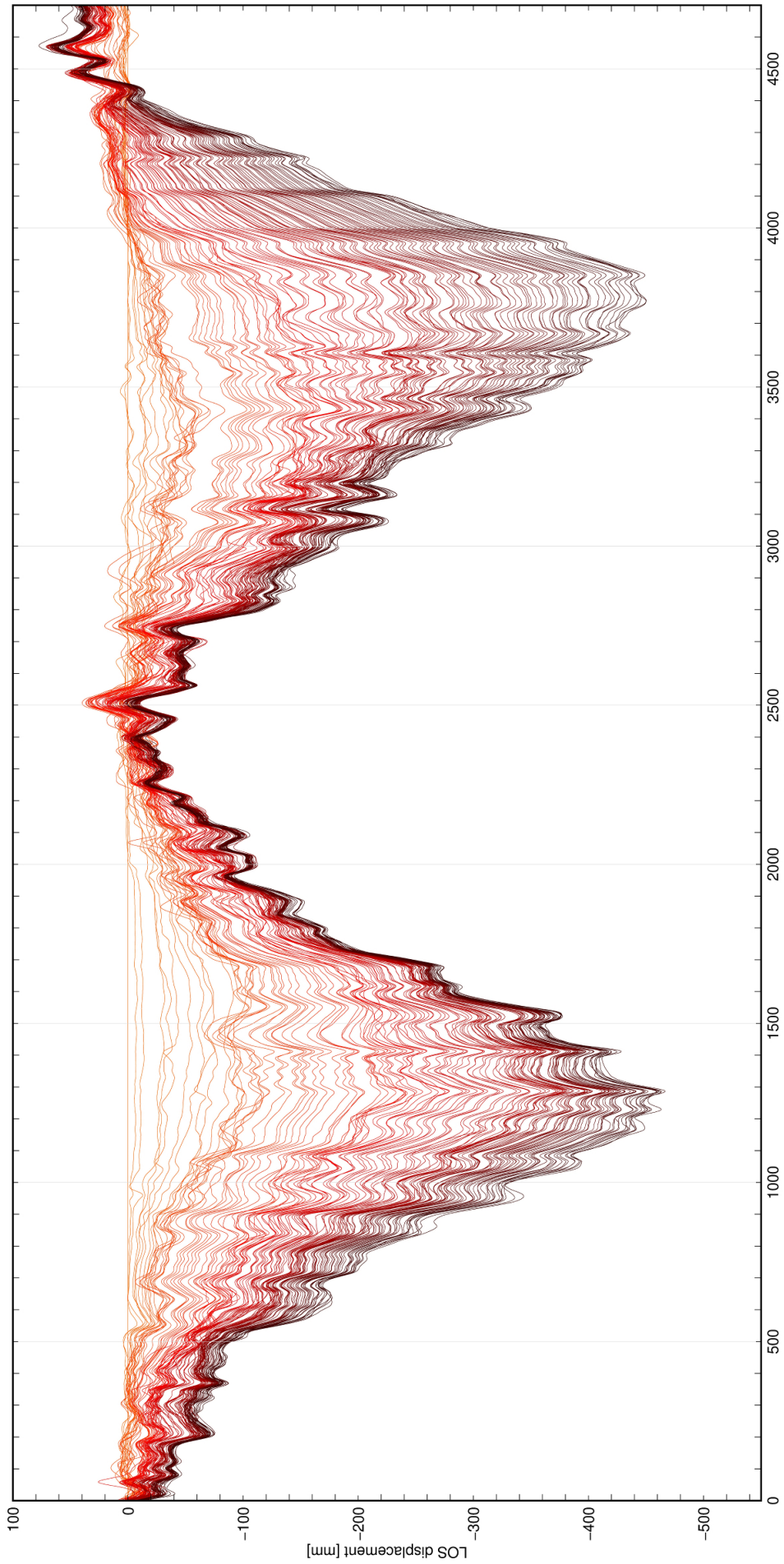

Fig. 16: Subsidence determined for the selected profile (highlighted in Fig. 15). Subsequent curves represent increases in shipments from a six-day interval(**01**).

SBAS calculations of the data obtained from the Sentinel 1A/B satellites allowed identification of 27 regions in which underground mining activity influences the ground surface. The presented results for the complete period subjected to analysis clearly demonstrate that the influence of underground mining on the surface is constant in time. Analysis of the displacements indicates regions in which successive curves intersect. In some locations, especially those in which the observed subsidences are small-scale, subsidence increments are inconsistent. In the majority of the graphs, however, successive curves have similar shapes, with a certain offset. When compared to the results from the Turow brown coal mine, the results from the LGCB region have much higher quality. I use these results to prove that SAR data and the method are useful in monitoring this type of phenomena on the ground surface.

Summary
The results of my research for both mining and post-mining areas demonstrate that synthetic aperture radar interferometry may be used in this type of regions. The presented results covering the Walbrzych region, as well as the Turow brown coal mine and the LGCB regions, constitute a significant contribution to the application of synthetic aperture radar interferometry in mining areas. In the case of the three above regions, the common denominator lies in demonstrating state-of-the-art SAR data to be an important source of additional information on the influence of mining activity on the ground surface.

On the other hand, my calculations also proved that in the case of displacements which are relatively small in time, the results obtained from InSAR methods may include significant error. In accordance with equation (1), errors related to the passing of the signal through the ionosphere and the troposphere can be separated from the interferometric phase. Publication (**O3**) in the series, which discusses inter alia estimation of atmospheric delays, is thus believed to be an important contribution to research in this field.

Develop a method for simultaneous estimation of the influence of tropospheric and ionospheric delay on the calculated SAR data

My displacement calculation results demonstrated that atmospheric delay in the interferometric phase may cause the detection of terrain surface changes to be impossible or significantly distorted. This fact remains of special importance in the case of surface changes which show limited amplitude and spatial range. As is the case with any measurement method, also the InSAR (DInSAR, PSInSAR or SBAS) methods have their significant limitations (Bürgmann et al., 2000). In the introduction, I mentioned that the topographic component and orbit errors may be calculated and separated in the interferometric phase. Unfortunately, thermal noise and dissipation variability constitute a component which is currently impossible to be eliminated. Atmospheric delay, which comprises ionospheric and tropospheric influences, is now the object of intensive research. After having passed through the atmosphere, the signal frequently does not allow detecting the expected deformations. In other cases, the atmospheric screen significantly distorts obtained results and prevents a reliable analysis of an event. For these reasons, the time and spatial variability of atmospheric conditions has the most significant influence on the accuracy of measurements performed using InSAR methods.

(**O3**) is the result of my research which started at the time of performing calculations for the regions of Walbrzych, the Turow brown coal mine, the Upper Silesian Coal Basin, the Bogdanka coal mine and the LGCB. My previous publications demonstrated that InSAR calculations may be significantly distorted due to the passing of the signal through the ionosphere and the troposphere. The above problem was the main motivation for interest in methods and techniques of calculating the tropospheric and ionospheric components from the interferometric phase. Literature studies (section 2 of the **O3** article) revealed that a large number of publications describes methods of eliminating the above mentioned components. Most of these methods are imperfect in that they allow estimation of only one of the two phase delays. At the same time, practically no publications discuss delay calculation in mining and post-mining areas. In my further research I decided to address these issues.

The approach of my proposal is new and consists in simultaneous allowance for the tropospheric

and ionospheric corrections in SAR data calculations based on the differential method (DInSAR). The new approach results from the combination of two methods:

- Generic Atmospheric Correction Online Service for InSAR (GACOS) (Yu et al., 2017, 2018) - for calculating tropospheric delay,
- Split-Spectrum (Rosen et al., 2010; Brcic et al., 2010; Gomba et al., 2016) - for calculating ionospheric delay.

Figure 17 shows a schematic diagram representing the implementation of Iterative Tropospheric Decomposition Model and Split-Spectrum Method for data obtained from the Sentinel satellites. Calculations of the tropospheric and ionospheric delays are independent. The delays are allowed for after the interferometer baseline phase is unwrapped and subsequently calculated into LOS displacements.

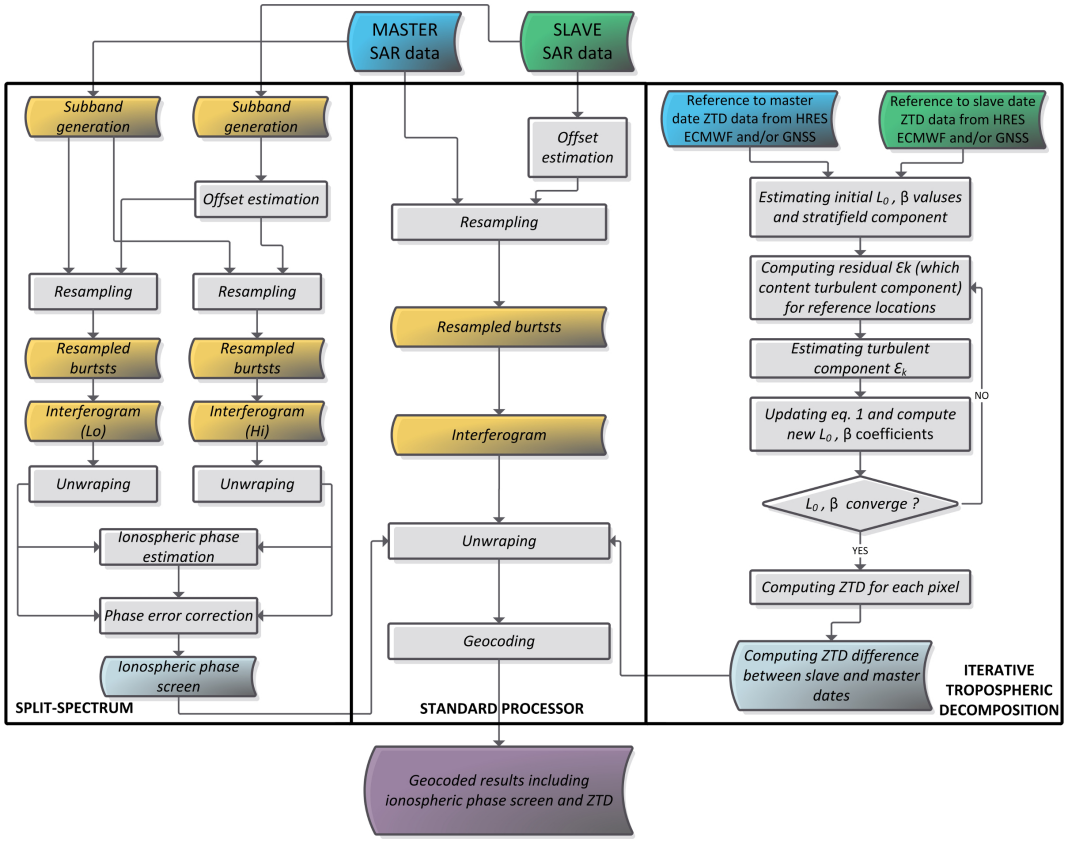

Fig. 17: Implementation of Iterative Tropospheric Decomposition model and split-spectrum methodin SAR calculations using the differential InSAR (DInSAR) method (Sentinel 1) (**O3**).

Tropospheric delay correction

The tropospheric influence was reduced by employing Generic Atmospheric Correction Model (GACOS), which is based on Iterative Tropospheric Decomposition Model (ITD). The ITD allows establishing zenith total delay (ZTD) for pixel k having a coordinate vector x (2), based on known ZTD values in reference points (HRES ECMWF and/or GNSS). The delay is calculated iteratively, by decomposing the signal into the stratigraphic and turbulent components (3).

$$ZTD_k = S(h_k) + T(x_k) + \varepsilon_k \tag{2}$$

where: S – stratigraphic component of tropospheric delay, correlated with height h, T – turbulent component and k – unmodeled part of the signal. The stratigraphic component is represented for any pixel by exponential function (4), and the values are interpolated using the inverse distance weighting (IDW) method.

$$S = L_o e^{-\beta h} \tag{3}$$

where: β is the exponential function coefficient, L_0 is the stratigraphic delay component at sea level; the above coefficients are determined using the smallest squares method, on the basis of the known ZTD values. The turbulent component is interpolated on the basis of a modified IDW method:

$$T = \sum_{i=1}^{n} w_{ui} T(x_i), \qquad w_{ui} = d_{ui}^{-2} / \sum_{i=1}^{n} d_{ui}^{-2} \tag{4}$$

where: u and i represent respectively: the location, for which T is calculated and a reference location of known T, w_{ui} is the weight of delay T, an interpolation coefficient dependent on the horizontal distance between the interpolated point and the reference point d_{ui}.

$$\begin{bmatrix} T_1 \\ T_2 \\ ... \\ T_n \end{bmatrix} = \begin{bmatrix} 0 & w_{12} & ... & w_{1n} \\ w_{21} & 0 & ... & w_{2n} \\ ... & ... & 0 & ... \\ w_{n1} & ... & w_{n,n-1} & 0 \end{bmatrix} \begin{bmatrix} \varepsilon_1 \\ \varepsilon_2 \\ ... \\ \varepsilon_n \end{bmatrix} \tag{5}$$

In the first iteration of equation (3), the turbulent component assumes a value of zero, and the delay it causes remains within the range of the unmodeled part of the signal k. The turbulent component is calculated independently from the unmodeled part of the signal, from equation (6), with allowance for the weights of equation (5). The determined turbulent component is introduced into equation (3) and coefficients L_0 and β are calculated again. The iterative process is continued for as long as is necessary for coefficients L_0 and β to converge to a certain value.

Ionospheric delay correction

The interferometric phase may be described with equation (6), which includes a dispersive and a non-dispersive component.

$$\Delta\phi = \underbrace{\frac{4\pi f_0}{c}(\Delta r_{topo} + \Delta r_{defo}}_{non-dispersive} + \underbrace{\Delta r_{tropo}) - \frac{4\pi K}{c f_0}\Delta TEC}_{dispersive} \tag{6}$$

where: f_o is the carrier frequency, Δr_{topo}, Δr_{defo} and Δr_{tropo} are respectively the topographic and the deformation components, and the opographic path delay, K is a constant equal to $40.28 \frac{m^3}{s^2}$, ΔTEC is the difference TEC between two acquisitions.

Unlike the troposphere, the ionosphere is a dispersive medium. This fact allows the ionospheric component to be isolated from the remaining part of the signal.

$$\begin{aligned} \Delta\phi_L &= \Delta\phi_{non-disp}\frac{f_L}{f_0} + \Delta\phi_{iono}\frac{f_0}{f_L} \\ \Delta\phi_H &= \Delta\phi_{non-disp}\frac{f_H}{f_0} + \Delta\phi_{iono}\frac{f_0}{f_H} \end{aligned} \tag{7}$$

Transformation of equation 7 for the interferograms for the two subranges produces equations which are the sum of dispersion $\Delta\phi_{iono}$ and non-dispersion components $\Delta\phi_{non-iono}$ equation (8).

$$\begin{aligned} \Delta\hat{\phi}_{iono} &= \frac{f_L f_H}{f_0(f_H^2 - f_L^2)}(\Delta\phi_L f_H - \Delta\phi_H f_L) \\ \Delta\hat{\phi}_{non-disp} &= \frac{f_0}{(f_H^2 - f_L^2)}(\Delta\phi_H f_H - \Delta\phi_L f_L) \end{aligned} \tag{8}$$

The implementation of the method proposed by me concerns the SAR calculations using the differential method (DInSAR). In order to show the impact of the reduction of atmospheric delays, I chose three induced seismic events from the LGCB area. Due to the fact that the Sentinel 1A/B satellites work on the C-band wave, which is much more "resistant" to the ionosphere than the L-band wave (GNSS) as an additional example I used data from the ALOS-1 satellite operating in the band L. Data from ALOS-1 temporarily included a series of earthquakes that occurred off the coast of Chile in 2010.

Tab. 2: Scene-acquisition basic information (**O3**).

Date and time of event (UTC)	type	strength [M_w]	event location	satellite	master Date and time (UTC)	slave Date and time (UTC)	path
11/29/2016 8:09:39 PM	Induced tremor	4.2	Poland, the LGCB region	Sentinel 1A	11/28/2016 4:43:20 PM	12/10/2016 4:43:20 PM	73
12/7/2017 5:42:50 PM	Induced tremor	4.5		Sentinel 1A/1B	12/5/2017 4:43:33 PM	12/11/2017 4:42:51 PM	
1/29/2019 12:53:45 PM	Induced tremor	4.1		Sentinel 1A/1B	1/26/2019 5:09:03 AM	2/1/2019 5:08:27 AM	22
3/11/2010 2:55:27 PM	Natural earthquake	7.0	Chile, Cardenal Caro province	ALOS 1	3/9/2010 4:03:29 AM	4/24/2010 4:03:06 AM	114
					3/9/2010 4:03:03 AM	4/24/2010 4:03:15 AM	

Such events can be observed in the interferometer phase as long as they are strong enough and if there are permanent displacements on the surface. In view of the above, I analyzed three induced seismic events (Tab. 2), which occurred in 2016, 2017 and in 2019. Each of the shocks had a magnitude greater than M_w 4.0.

Detection of the impact of mining tremor is the subject of the third specific objective presented later in the self-review.

In accordance with the proposed calculation procedure (Fig. 17) the ITD model was used to calculate the tropospheric delay difference for each SAR pair. The delay range for the analyzed LGCB area in successive periods was, respectively [mm]: -31/54 (2016), -4/27 (2017) and -22/10 (2019). Analyzing the changes observed on the profiles, I found that the inclusion of amendments significantly improved the final results. After applying the corrections, it is possible to observe two significant changes. Firstly, local displacement variations became significantly reduced. The displacements in the profile are more gentle. Secondly the growth from the north to the south is eliminated. The observed tremor location did not change after applying corrections. The correction resulted in a slightly reduced maximum of the subsidence trough.

The comparison (Fig. 21) indicates that the ionospheric correction significantly reduces local variation. The result of its application is best illustrated in the comparison of displacements for the first analyzed period. This fact is best seen in the case of the 2017 even and of the 2010 earthquake. Examples from the LGCB area show that the global (i.e., in the entire analyzed range - length of the profile) the ionospheric correction share is much smaller compared to the tropospheric correction values. Taking into account the influence of the troposphere improves the results of dislocations in such a way that they are in fact an "screen" of initial displacements (with minimized local variations) transformed by a vertical vector. This is very clearly visible in the case of the 2017 event and the 2010 earthquake.

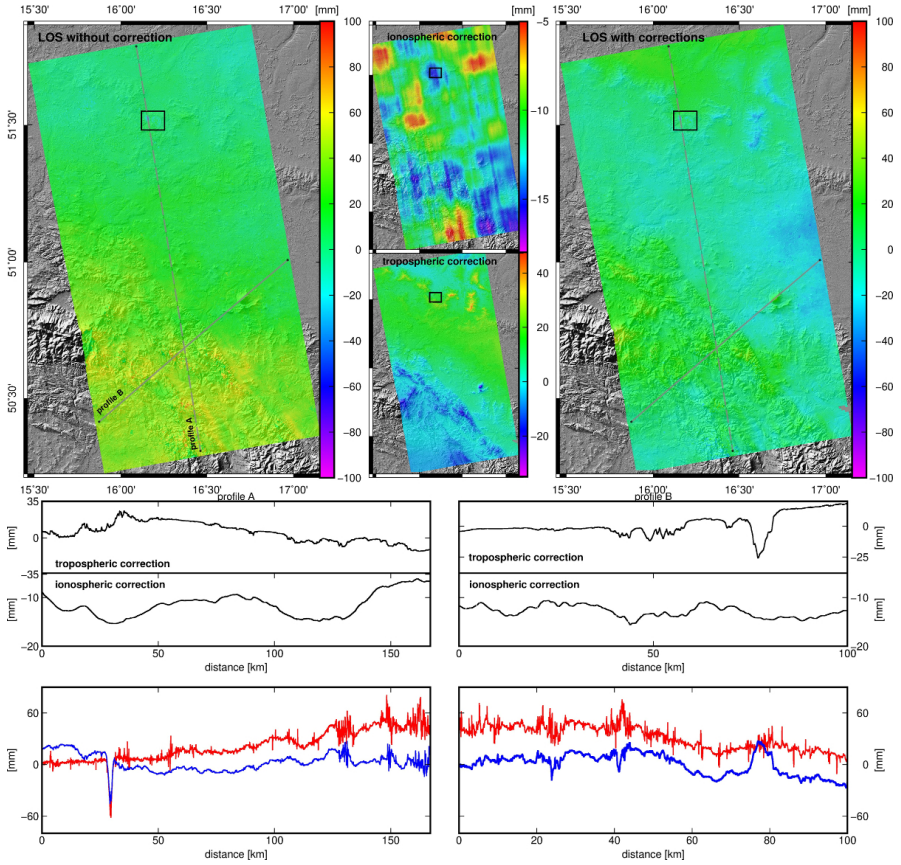

Fig. 18: Results for the 2016 tremor. (left) LOS displacements calculated with the use of the DInSAR method (Sentinel 1, TOPS) for period of 28 November 2016–10 December 2016. Calculated values: (middle-top) ionospheric component, (middle-bottom) tropospheric component, and LOS displacements allowing for the above components. Graphs: Calculated values: ionospheric componentand tropospheric component for each of the cross-sections (top). Comparison of results without allowance for corrections (red line) and with allowance (blue line) for ionospheric component and tropospheric component (bottom) (**O3**).

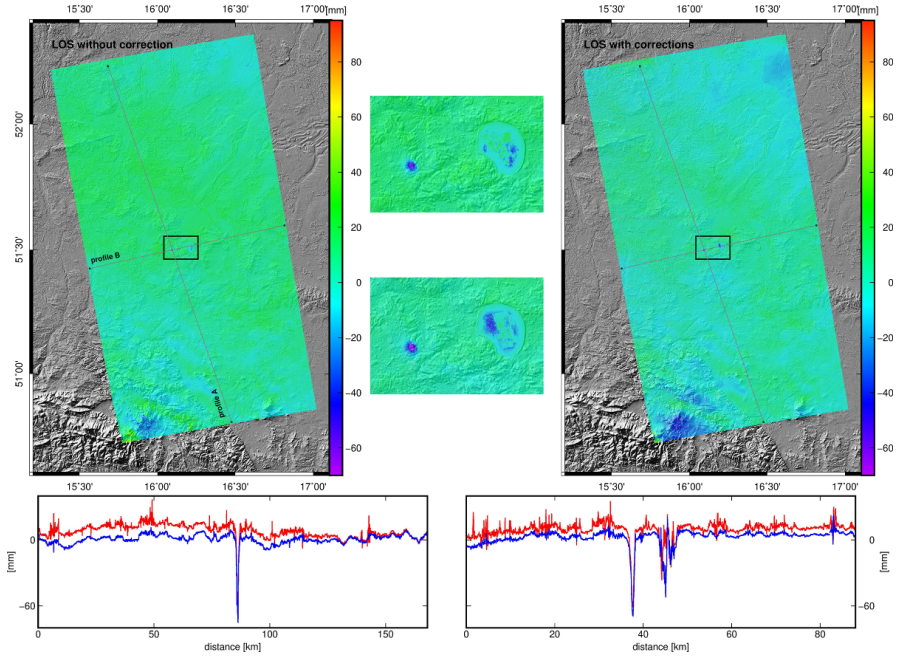

Fig. 19: Results obtained for the 2017 tremor, LOS displacements calculated with DInSAR (Sentinel1, TOPS) for (left) the period of 12 May 2017–11 December 2017; (right) LOS displacements with allowance for the influence of the ionosphere and the troposphere. Red line indicates displacements without allowance for corrections, and blue line with allowance for corrections (**O3**).

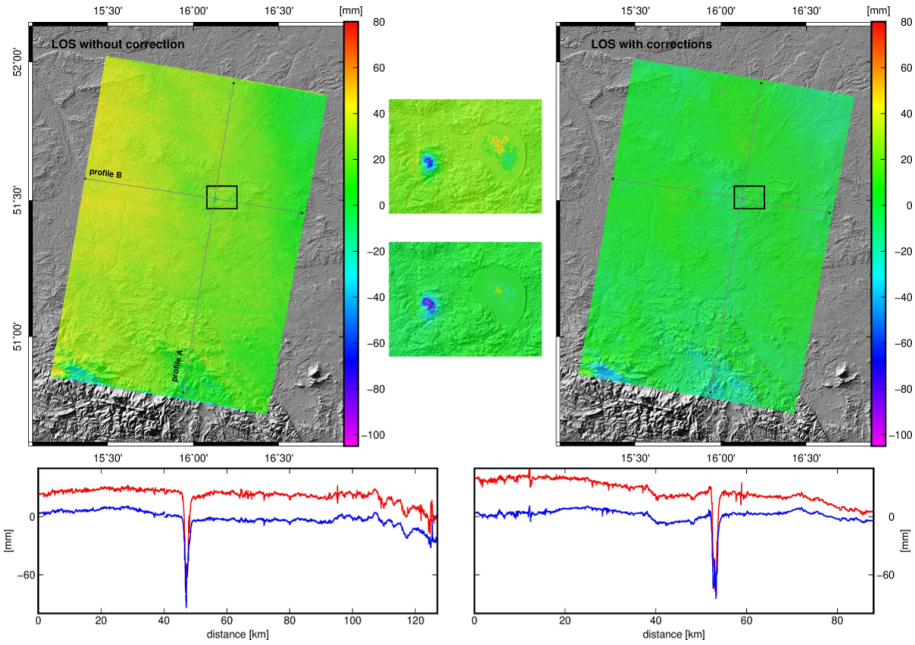

Fig. 20: Obtained results for the 2019 tremor, LOS displacements calculated with DInSAR (Sentinel1, TOPS) for (left) the period of 26 January 2019–2 February 2019; (right) LOS displacements with allowance for the influence of the ionosphere and the troposphere. Red line indicates displacements without allowance for corrections, and blue line with allowance for corrections (**O3**).

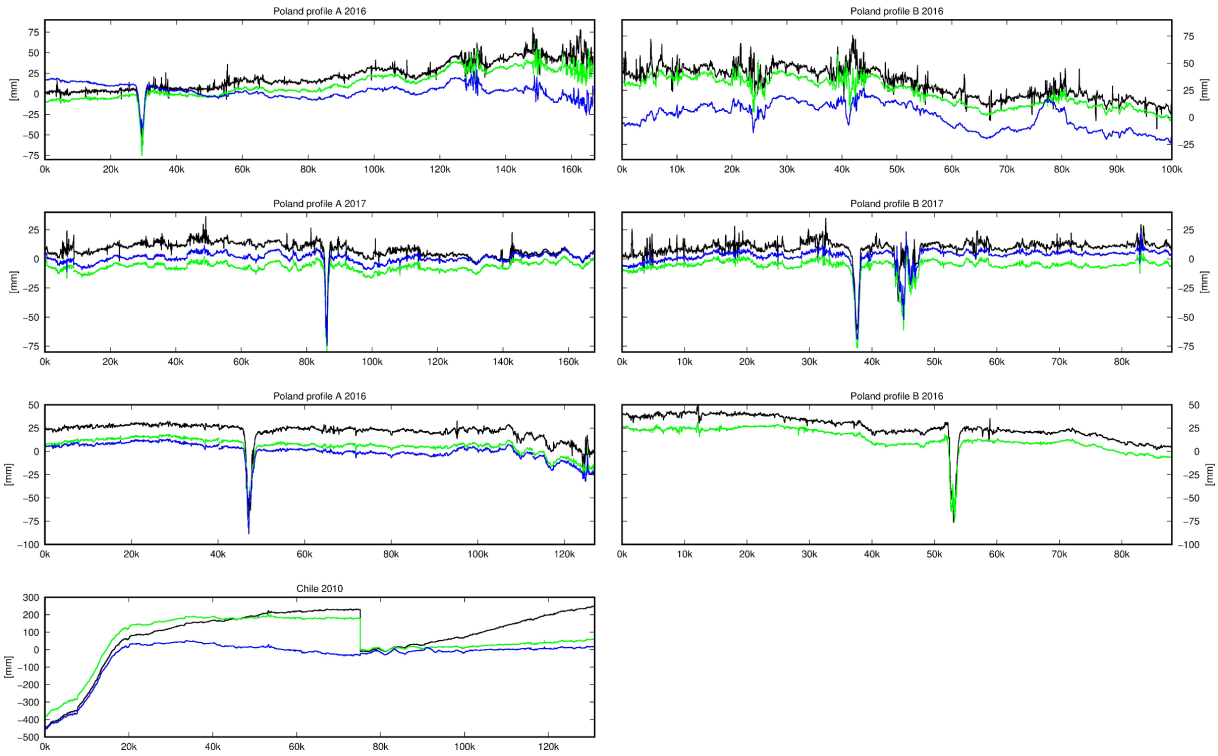

Fig. 21: Comparison of observed displacement fluctuations in the profiles. Black line denotes the original data; green line, results including ionospheric correction; blue line, results including both ionospheric and tropospheric corrections (**O3**).

The possibility of applying InSAR methods in the detection of induced seismic events in mining areas.

Articles (**O1** and **O2**) relate to the use of DInSAR and SBAS methods in tracking the impact of mining shocks on surfaces.

Research to date has shown that Synthetic Aperture Radar (SAR) interferometry may be successfully used in the measurements of the influence that earthquakes have (on a regional scale) on a land surface (Tong et al., 2013; Tung and Masterlark, 2016). SAR interferometry is also used to estimate the activity of tectonic faults (Chaussard et al., 2014; Hussain et al., 2016) and volcanic activity (Henderson and Pritchard, 2013; Remy et al., 2015; González et al., 2015). The factors that influence the induced seismic events are: the depth of exploitation, the type of exploitation system, as well as geological and mining conditions (Gibowicz and Kijko, 1994). Mining tremors are generated when mining stresses, tectonic stresses and lithostatic stresses overlap. These stresses cause an increase of the potential energy in the rock mass. When the strength limits are exceeded, the rock mass is destroyed and the potential energy is rapidly released. Tremors accompany mining operations in many mining basins all around the world, e.g.. in Great Britain (Kusznir et al., 1980), in Germany (Bischoff et al., 2010), in the Republic of South Africa (Riemer and Durrheim, 2012), in the United States (Kubacki et al.), in China (Wang et al., 2015), or in Poland (Drzewiecki and Piernikarczyk, 2017). Threats related to mining tremors represent the most serious hazards in mining operations. In Poland, the problem of mining tremors is related to underground mining carried out in the Upper Silesian Coal Basin and in the LGCB, as well as in the open cast lignite mine in the Belchatow Lignite Basin. The occurrence of a mining tremor may lead to permanent changes on the surface. These changes may take the form of local land depressions or discontinuous deformations in the form of cracks, roofs, thresholds, etc. The deformations created on the surface are measured using traditional geodetic measurements and GNSS measurements. Nevertheless, in recent years, attempts have been made to use satellite radar data to detect such phenomena on the surface (Malinowska et al., 2018; Milczarek, 2019).

Article (**O2**) is an attempt at using synthetic aperture radar interferometry to determine surface displacement in a region affected by a strong induced earthquake caused by underground mining operations. The tremor I analyzed in this paper occurred on November 29, 2016. I assumed that the satellite radar data obtained from the Sentinel 1A/B satellites may be used to monitor induced seismicity, i.e. mining tremors. Such seismic activity is observed at much smaller depths, and the surface area affected by such activity is much more limited than in the case of natural seismic events.

In the first place, I conducted an analysis of the impact of mining shock based on radar data from Sentinels 1A and 1B (tab. 3, Fig. 22). Due to the fact that copper ore is exploited in the

Tab. 3: Interferograms used in the analysis of the Nov. 28, 2016 * - mining tremor, together with basic information (**O2**)

track no.	Satellite	Reference Date/ Product/Time of acquisition (UTC) **	Repeat Date Product/ Product/Time of acquisition (UTC) **	Flight direction	B. perp (m)	Mean Coherence [-]
22	Sentinel 1B	19.11.2016/05:08:34	01.12.2016/05:08:34	Descending	127	0.37
22	Sentinel 1B	01.12.2016/05:08:34	13.12.2016/05:08:34	Descending	14	0.29
73	Sentinel 1A	16.11.2016/16:38:23	28.11.2016/16:38:23	Ascending	42	0.35
73	Sentinel 1A	28.11.2016/16:38:23	10.12.2016/16:38:23	Ascending	-51	0.44
73	Sentinel 1B	22.11.2016/16:38:25	04.12.2016/16:38:25	Ascending	-6	0.41

* The analyzed tremor took place at 20:09:39 UTC

** Time of acquisition in this case means the end of data acquisition for the IW2 sub–swath; in the case of all SAR images used, mean measurement time for the whole IW2 was 31 s.

area of the tremor, I had decided to carry out additional calculations using the SBAS time series method. The calculation period covered the entire year 2016. A total of 27 SAR images (Sentinel 1A and 1B) from track no. 73 were used for the calculations (Fig. 24). The average period between each acquisition was 12 days. The total number of interferograms was 78. I had assumed that calculations using the SBAS method would allow the exploitation impacts on the surface to be correlated with the shifts that exposed the analyzed tremor. Additionally, in the SBAS calculations, I used the

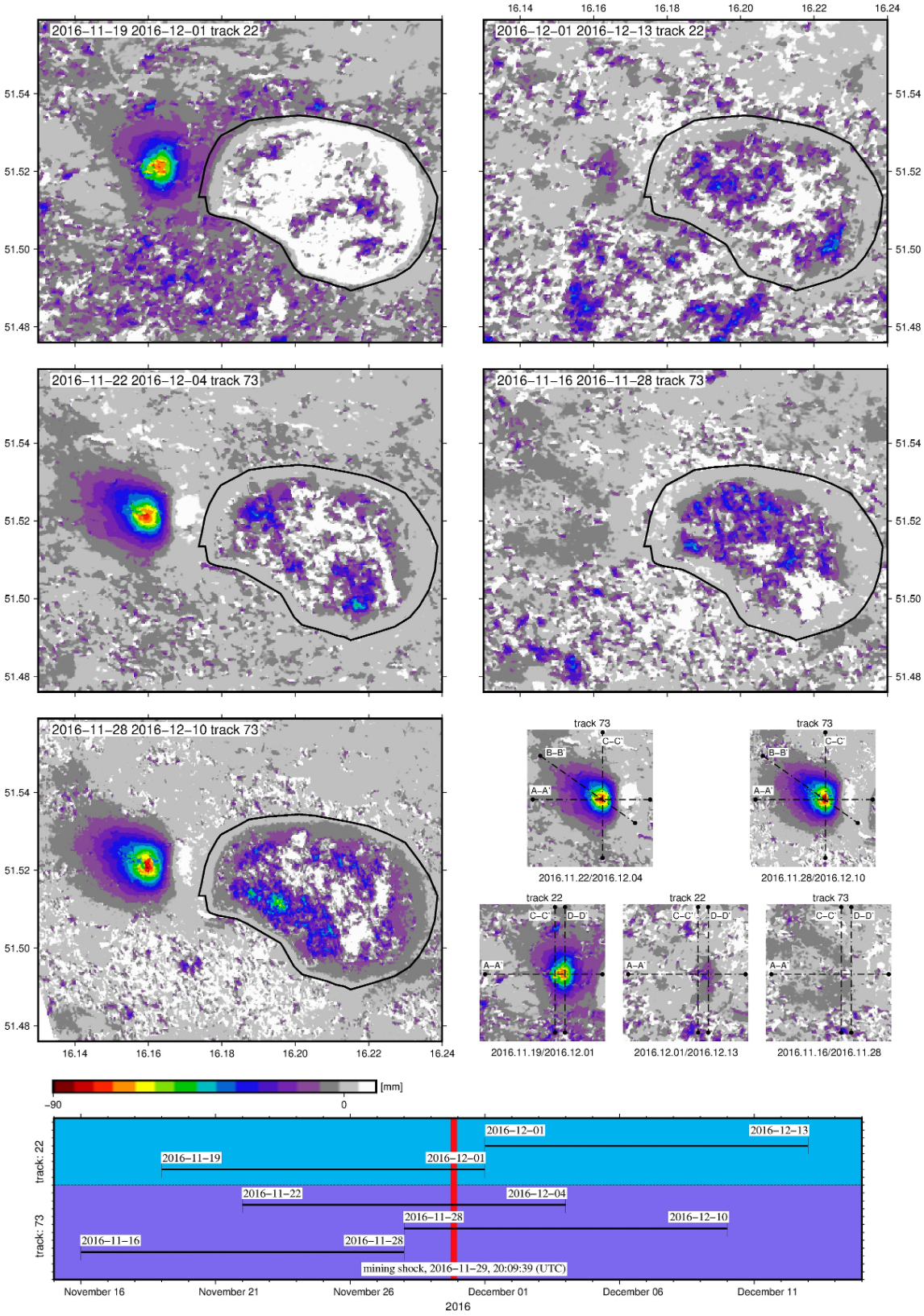

Fig. 22: The LOS displacements (in mm) calculated from subsequent interferograms The five main maps include,in their top left corners, the dates of the SAR images used for displacement calculations. The black contour denotes the Żelazny Most post–flotation tailings reservoir. On the right, the location of subsequent profiles is provided: A–A', B–B', C–C', D–D'. The bottom part of the image shows the distribution of subsequent interferograms in time, with regard to the date of the mining tremor (the red vertical line) (**O2**).

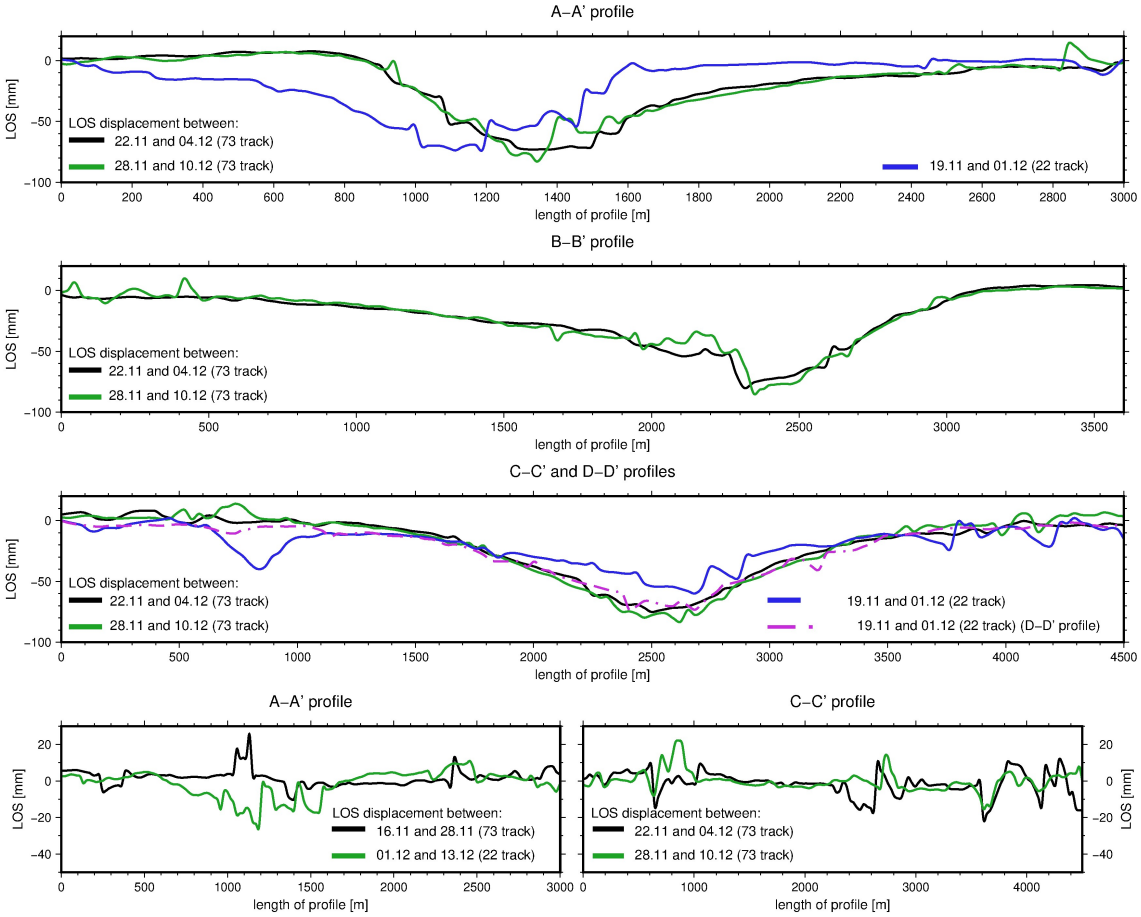

Fig. 23: Profiles of the slopes in the region of the trough created by the induced tremor The A-A' profile is oriented in the E-W direction, the B-B' profile-in the NW-SE direction, the C-C' and the D-D' profiles-in the N-S direction. The shift of the D-D' profile in relation to the C-C' profile is 445 m (**O2**).

empirical model of atmospheric reduction proposed by Tymofyeyeva and Fialko (2015). The results obtained by the SBAS method (Fig. 24) indicate that in the mining tremor region a subsidence basin has been formed during the whole 2016. In the period between November 28 and December 10, there was a sharp subsidence in the tremor area of the whole year. The maximum subsidence observed on the A–A and C–C profiles was approximately -80 mm (Fig. 23). SBAS results are consistent with previously presented results obtained by the DInSAR method. The spatial range of subsidence of the tremor coincides with the existing mining subsidence basin.

The obtained results showed the possibility of detecting land surface changes as a result of a strong mining tremor (induced event) based on radar data from Sentinel 1A/B satellites.The distinguishing feature of the results obtained in relation to other items (Barnhart et al., 2014) is the range of detected changes. Although an attempt was made to observe surface displacements accompanying the Dec. 26 2016, tremor, no significant additional surface displacements were identified either before or after the analyzed tremor occurred. The SBAS calculations clearly showed that the observed displacements coincide with the subsidence basin which is connected with the underground exploitation of copper ore conducted in this area. On this basis, it can be concluded that the induced mining tremor can promote affect the deformation of the ground surface in the area of exploitation. The location of the tremor occurred exactly in the operating field XXI2 (unit branch G–23) which additionally confirms the induced character of the shock.

Continued research into the application of SAR data to the analysis of the influence of mining tremors on the ground surface resulted in article (**O1**), which is the last position in the publication series. This manuscript is also a summary of my research into the possibility of applying InSAR methods in the detection of induced seismic events in mining areas.

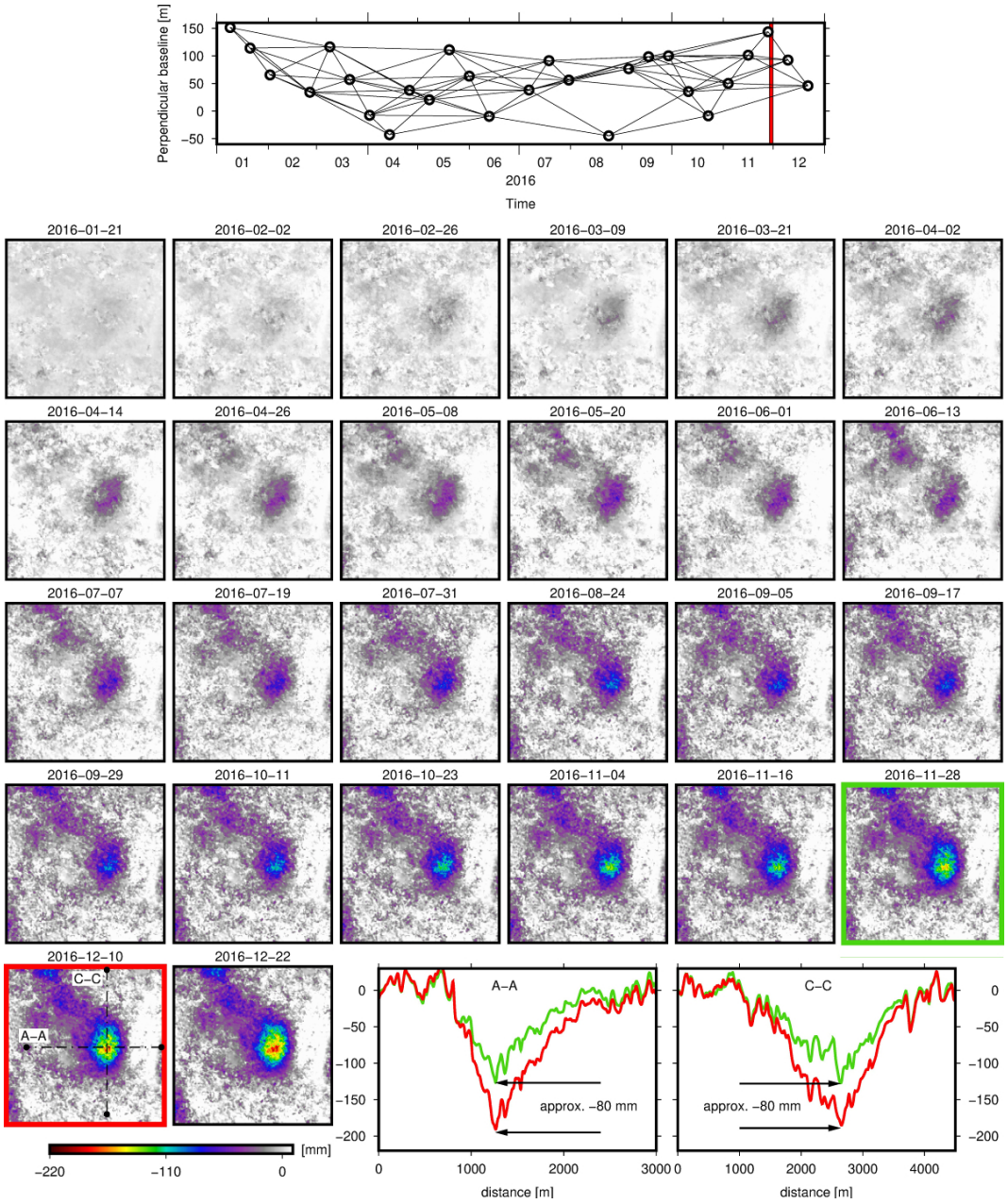

Fig. 24: LOS dislocations were determined on the area of the analyzed mining tremor based on the SBAS method. At the top, a combination of 78 interferograms calculated for the entire 2016 was presented. The date of the tremor was marked with the red line. The next LOS displacements (in mm) in 2016 were presented for 26 periods. Maps with green and red envelopes indicate the periods immediately before and after the tremor of November 2016. The diagrams show the displacements for the same cross-sections (A-A and C-C) as for the DinSAR calculation (**O2**).

The main purpose of the research presented in (**O1**) was to verify whether synthetic aperture radar interferometry may be successfully employed in long-term analyses of surface displacements in mining areas. I also presented the possibility to use the empirical method for atmospheric delay estimation, as proposed by Tymofyeyeva and Fialko (2015), to indirectly detect induced tremors.

The main assumption of this method is that two (or more) interferograms that have a common scene contain the same (in terms of value) atmospheric component of the phase resulting from propagation of the troposphere and ionosphere wave. In the drawing 25 I presented the basic assumptions of the method. Let us assume that we have two interferograms calculated on the basis of three images (in such case the acquisition times are t_1, t_2 and t_3, respectively - Figure 25). In

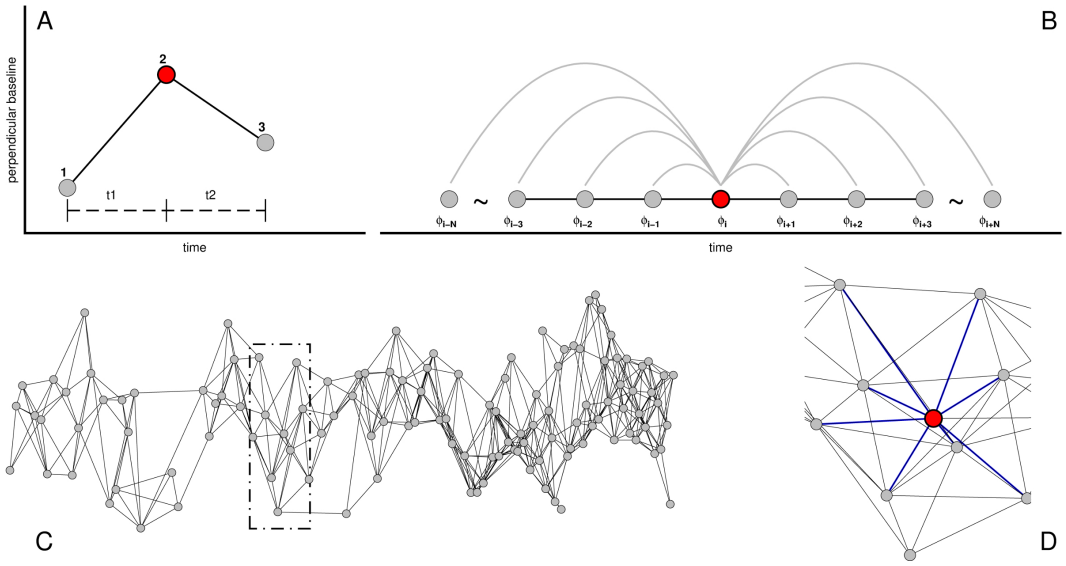

Fig. 25: Graphic representation of the basic assumptions behind the method. Part A shows two interferometric pairs having one common image (number 2, denoted in red color). Part B represents the idea behind the method: the more pairs of SAR images with the same recurring image (in red), the more accurate the estimation of atmospheric correction for the image (date). Part C shows the baseline plot for the analyzed SAR data from path 73. Part D, on the other hand, shows the actual implementation of the model. Parts A and B are based on Tymofyeyeva and Fialko (2015) (**O1**).

the case of each interferogram, the equations will have the following form, respectively:

$$\Delta\phi_{12} = \Delta\tau_{12} + \alpha_2 - \alpha_1 + \varepsilon_{12} \quad \text{and} \quad \Delta\phi_{23} = \Delta\tau_{23} + \alpha_3 - \alpha_2 + \varepsilon_{23} \tag{9}$$

where α_i – atmospheric component due to signal propagation among others in the atmosphere and in the ionosphere, in time t_i and $\Delta\tau_{ij}$ is the phase component related to the observed ground surface deformations in time t_{ij}.

Accordingly, it is possible to designate the phase component, which is responsible for the propagation of the signal on a given day (day data acquisition). At this stage, an additional assumption should be formulated that the $\Delta\phi_{12} - \Delta\phi_{23}$ difference is independent of the deformation component on condition that the time base is constant and deformation increments are constant in time. This assumption is of key importance for the results presented in this paper. It is also similar to the properties of other empirical methods employed to eliminate atmospheric delays in InSAR calculations Bekaert et al. (2015). The generalized formula for the atmospheric component in the form of (10):

$$\alpha_i = \lim_{N\to\infty} \frac{1}{2N} \sum_{j=1}^{N} \Delta\phi_{i(i-j)} - \Delta\phi_{(i+j)i} = \lim_{N\to\infty} \frac{1}{2N} \sum_{j=0}^{N-1} (N-j)[\Delta\phi_{(i-j)(i-j-1)} - \Delta\phi_{(i+j+1)(i+j)}] \tag{10}$$

I performed a series of test calculations to verify the potential of the method advanced by (Tymofyeyeva and Fialko, 2015) . I based the SBAS calculations on theoretical data prepared with the use of the Mogi model. It is an analytical model, which describes the magnitude and the direction of ground displacements due to changed volume or pressure of a point in a uniform elastic half space (Fig. 26). This approach allowed simulating both underground mining exploitation and induced tremors. The application of the Mogi model and test calculations was aimed at identifying how the empirical model of atmospheric delay estimation influences the displacement results in the case of an induced tremor. With regard to the time-constant displacement assumption behind the model, I verified whether a signal caused by a mining tremor may be also identified. If so, the model proposed by Tymofyeyev and Fialko could be applied to directly estimate the influence of mining tremors on ground surfaces. Detection of mining tremors in actual conditions with the use of SAR data is

frequently hindered by the fact that intensive mining on a large area (e.g. the LGCB area) causes numerous surface subsidences (the so-called subsidence troughs) to occur locally. In the majority of cases, the influence of a mining tremor is observed within the borders of the existing subsidence troughs. This fact is an additional difficulty in determining the impact of mining tremors on surfaces.

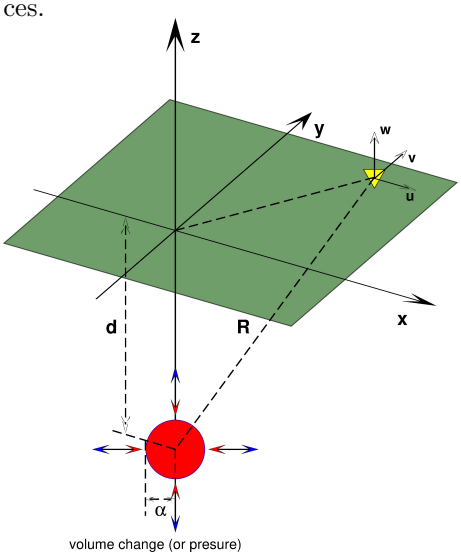

$$\begin{pmatrix} u \\ v \\ w \end{pmatrix} = \Delta V \frac{(1-\nu)}{\pi} \begin{pmatrix} x/R^3 \\ y/R^3 \\ z/R^3 \end{pmatrix} \tag{11}$$

Fig. 26: Schematic diagram of the Mogi model (**O1**)

In the test calculations I have created 24 time periods ($t_1 \ldots t_{24}$) between which time-constant ground surface subsidences of -40 mm occurred due to mining activity at a depth of 500 m. The time interval between the periods was constant. Figure 27 shows baseline plot for the test data. The spatial range of the test data was 10x10 km.

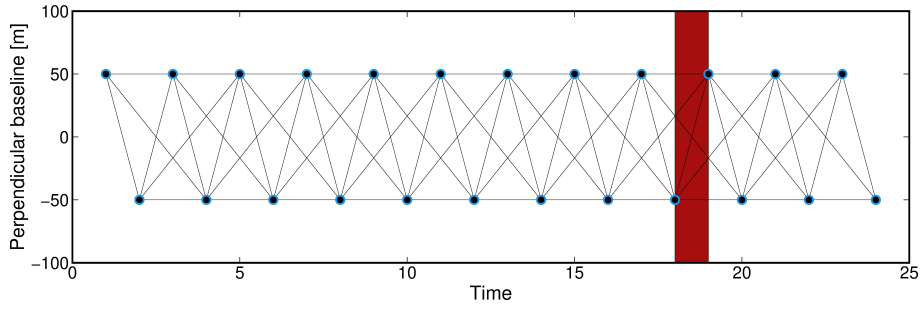

Fig. 27: Temporal and perpendicular baselines of the final selected pairs of hypothetical SAR datas (**O1**).

Based on the defined assumptions, three independent calculation cases were prepared:

(I) mining activity without a mining tremor,

(II) mining activity with a mining tremor recorded between t_{18} and t_{19}, the tremor having occurred exactly in the center of the already existing subsidence trough,

(III) mining activity with a mining tremor recorded between t_{18} and t_{19}, but unlike in case (II) the tremor occurred outside the mining area influenced by mining operations and was located at a distance of approximately 3 km from the center of the already existing subsidence trough.

In the first case, without a mining tremor, maximum ground subsidence was -969 mm. Figure **??** shows subsidence increments along a selected profile and allows an observation that increments are constant between subsequent periods. As is expected, no significant values of atmospheric component are observed. In the second analyzed case (Fig. 29), a tremor was assumed in the period between t_{18} and t_{19}. In this scenario, total subsidence was -1150 mm. The graph (Fig. 29, right-hand side, in the middle), shows the values of the determined atmospheric corrections. Corrections having maximum values between -90 and +75 mm were observed in the periods directly before and after the tremor (t_{18} and t_{19}). Another observation points to the fact that significant values of atmospheric corrections occur in all data which formed interferometric pairs with the t_{18} period. At

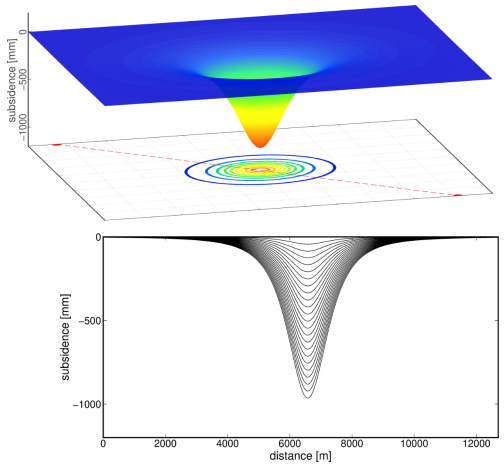

Fig. 28: Results of test calculations with the SBAS method for 24 periods. Subsidences were simulated on the basis of the Mogi model. The figure shows a subsidence trough for the first analyzed case without an induced seismic event. The graph in the bottom shows increment dynamics of the simulated ground surface subsidences. The dashed red line indicates the profile (**O1**).

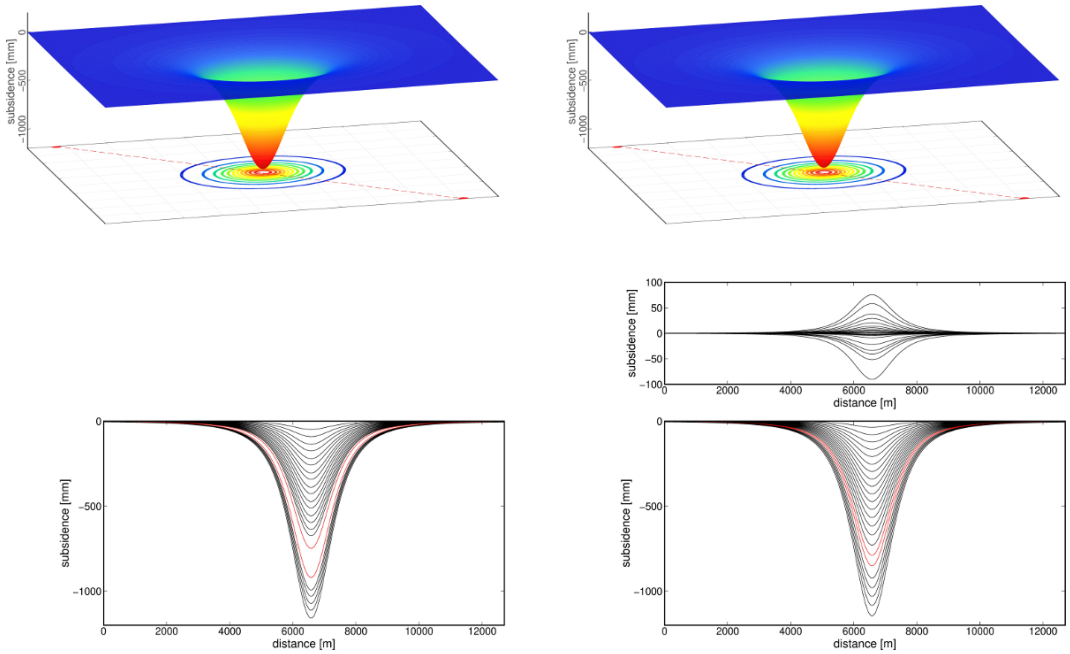

Fig. 29: On the left-hand side: results for the case involving a mining tremor which occurred in the period between t_{18} and t_{19}, without the model of atmospheric component reduction. On the right-hand side: the same case, but with the reduction model. The graph in the middle (on the right) represents the values of atmospheric components. The graphs in the bottom show increment dynamics of the simulated ground surface subsidences. The dashed red line indicates the profile. (**O1**).

the same time, the value of the subsidence between periods t_{18} and t_{19} was -61 mm. The third case also involved a mining tremor between periods t_{18} and t_{19}. While in the previous case the tremor was located exactly in the already existing subsidence trough, the tremor in this scenario occurred outside the surface area influenced by mining activity (Fig. 30).

This empirical method has been successfully used in areas demonstrating displacements which are constant in time (Xu et al., 2017). Like some other empirical methods Bekaert et al. (2015), this method does not work well in the case of sudden events (outlying events), such as mining tremors. Figure **??** shows an example of how the method is applied in an area, in which time-constant displacements are accompanied by sporadic sudden events. The results here presented relate to the test models described above. Time-constant ground displacements determined with the SBAS

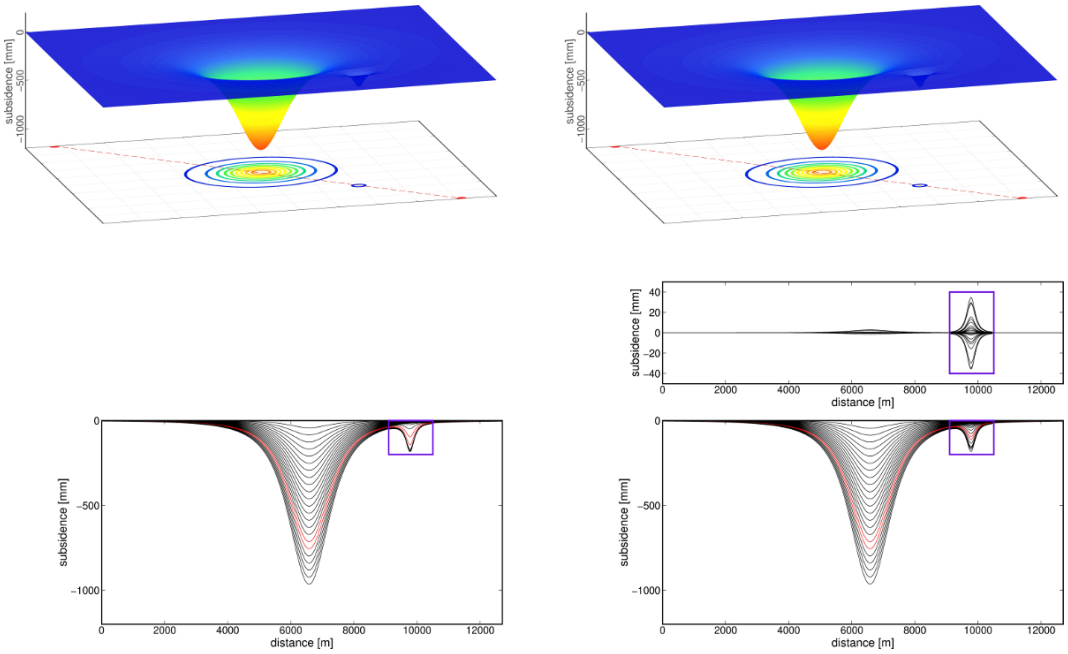

Fig. 30: Results of the third test case which involved a mining tremor located outside the surface area influenced by mining activity. The results without and with allowance for atmospheric correction, on the left-hand side and on the right-hand side, respectively. The dashed red line indicates the profile and the location of the tremor is indicated with the violet polygon (**O1**).

method without the model are correct (i.e. they show as time-constant subsidence increments). The situation is different in the case when an event results in greater displacements observed on the surface. In such case the model reduces the displacement values to approximate the level from the periods when surface displacements were constant. As a result, displacement analysis cannot be used to identify tremor location. In such situation, the results are not fully reliable. The time of the tremor may be identified only by analyzing the atmospheric component. Interestingly, upon comparison, the calculated total displacement values show to be practically identical for cases in which tremors are analyzed with and without allowance for the reduction model (Fig. 31).

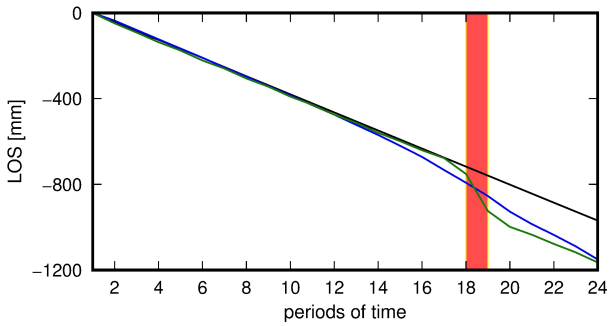

Fig. 31: Results of test calculations – displacements of the point in the central part of the subsidence trough. The black line represents displacements in the first case (see section 5.1), without the mining tremor and with the atmospheric component reduction model. The green line represents displacements in the second case, with the mining tremor and without the atmospheric component reduction model. The blue line represents displacements in the third case, with the mining tremor and with the atmospheric component reduction model. The area denoted in red corresponds to the period in which the tremor was simulated (**O1**).

The obtained results showed that the application of the atmospheric delay reduction model in the SBAS calculations does not adversely affect the displacement results. On the other hand, on the basis of conducted test calculations, it was shown that in the case of an emergency (e.g. of a seismic nature) in the atmospheric component of the signal phase, in a sense, the image of the event itself is registered. (Fig. 29, 30).

My analysis of the results (Tab. 4, Fig. 32) showed that it is possible to observe an image of a shock in the determined atmospheric component. In the case of the LGCB area, the atmospheric delay reduction model applied allows in the majority of cases detection of induced shocks, the force of which is greater than M_w 4.1.

I identified a property of SBAS calculations with allowance for the empirical atmospheric delay estimation model which may be used in detecting the influence of mining tremors on ground surfaces. The analysis of the results proved that tremor detection based on SAR data obtained over a period greater than 6 – 12days is difficult due to the influence of mining activity observed in the signal phase. Figure 32 shows the results for three selected induced seismic events. The first two rows correspond to the same event. The first row represents SAR data results with the time base of 12 days. The results obtained in this case allow the tremor location to be identified precisely. The second row represents displacement results for longer time bases: 36 days (for track 22) and 24 days (for track 73). In the case of track 22, where the time base was over one month, additional subsiding troughs may be observed, which are the result of mining activity on the surface. Rows 3 and 4 present the results for selected tremors identified from SAR data with a time interval of 6 days. The test calculations performed with the use of the atmospheric delay reduction model

Tab. 4: Calculation results for 23 selected mining tremors which occurred in the LGCB region between 2014 and 2018 (**O1**).

date and time	**tremor**	**22**	**73**	**observed event**			
of event (UTC)	$[M_w]$	before ÷ after	before ÷ after	LOS		APS	
(Day/Month/Year)		(Day/Month/Year)	(Day/Month/Year)	22	73	22	73
05/05/2018-03:40:56 PM	4.0	01/05/2018 ÷ 07/05/2018	04/05/2018 ÷ 10/05/2018	-	-	-	-
14/04/2018-03:58:52 PM	4.1	13/04/2018 ÷ 19/04/2018	10/04/2018 ÷ 16/04/2018	-	-	-	-
26/12/2017-11:15:31 AM	4.5	26/12/2017 ÷ 01/01/2018	23/12/2017 ÷ 29/12/2017	+	+	+	+
07/12/2017-05:42:50 PM	4.1	02/12/2017 ÷ 08/12/2017	05/12/2017 ÷ 11/12/2017	+	+	+	+
10/11/2017-11:19:07 AM	4.3	08/11/2017 ÷ 14/11/2017	05/11/2017 ÷ 11/11/2017	+	+/-	+	+
27/10/2017-05:12:14 AM	4.0	27/10/2017 ÷ 02/11/2017	24/10/2017 ÷ 30/10/2017	+	+	+/-	+
31/05/2017-08:25:26 PM	4.5	30/05/2017 ÷ 11/06/2017	27/05/2017 ÷ 02/06/2017	-	-	-	-
08/04/2017-10:23:13 PM	4.3	31/03/2017 ÷ 12/04/2017	28/03/2017 ÷ 09/04/2017	+/-	+	+	+
17/03/2017-08:50:19 AM	4.2	07/03/2017 ÷ 19/03/2017	16/03/2017 ÷ 28/03/2017	+/-	+	+	+
04/03/2017-04:46:10 PM	4.1	23/02/2017 ÷ 07/03/2017	04/03/2017 ÷ 16/03/2017	-	-	-	-
16/12/2016-06:46:51 AM	4.6	13/12/2016 ÷ 25/12/2016	10/12/2016 ÷ 22/12/2016	+	+	+	+
29/11/2016-08:09:42 PM	4.5	19/11/2016 ÷ 01/12/2016	28/11/2016 ÷ 10/12/2016	+	+	+	+
17/10/2016-11:50:33 PM	4.3	14/10/2016 ÷ 26/10/2016	11/10/2016 ÷ 23/10/2016	+	+/-	+	+
14/09/2016-07:59:09 AM	4.1	14/19/2016 ÷ 26/09/2016	05/09/2016 ÷ 17/09/2016	-	-	-	-
13/08/2016-12:00:58 PM	4.3	09/08/2016 ÷ 21/08/2016	31/07/2016 ÷ 24/08/2016	-	-	-	-
02/06/2016-04:08:57 AM	4.0	29/05/2016 ÷ 10/06/2016	01/06/2016 ÷ 13/06/2016	-	-	-	-
11/05/2016-04:01:36 AM	4.0	23/04/2016 ÷ 17/05/2016	08/05/2016 ÷ 20/05/2016	-	-	-	-
09/09/2015-07:30:16 PM	4.0	08/09/2015 ÷ 20/09/2015	25/07/2015 ÷ 23/09/2015	-	-	-	-
19/07/2015-07:18:06 PM	4.2	10/07/2015 ÷ 22/07/2015	13/07/2015 ÷ 25/07/2015	-	-	-	-
08/07/2015-06:53:20 AM	4.4	28/06/2015 ÷ 10/07/2015	01/07/2015 ÷ 13/07/2015	-	-	-	-
05/02/2015-04:43:59 AM	4.0	04/02/2015 ÷ 16/02/2015	26/01/2015 ÷ 07/03/2015	+/-	+/-	+	+
28/01/2015-01:10:45 AM	4.3	23/01/2015 ÷ 04/02/2015	26/01/2015 ÷ 07/02/2015	-	-	-	-
12/12/2014-02:50:00 AM	4.1	06/12/2014 ÷ 18/12/2014	09/12/2014 ÷ 02/01/2015	+/-	+/-	+	+

the + sign indicates that a tremor was observed on an interferogram or on the atmospheric component. The - sign indicates that no tremor was observed. The +/- sign indicates that the occurrence of a tremor could be neither definitely confirmed nor definitely negated.

resulted in two observations which are of significance from the perspective of monitoring surfaces of mining areas. Firstly, if constant displacements occur in the analyzed area, then the application of the model does not have a significant effect on the scale of calculated displacements. Secondly, if a tremor occurs in a considered area, then the applied model reduces displacements due to the seismic event. Some values of these displacements are observed in the calculated atmospheric correction, related to images forming interferometric pairs. If a tremor occurs outside the area affected by mining activity, the displacement value is practically completely reduced. The image of such an event is recorded in the part of the signal corresponding to the atmospheric correction. Therefore, the

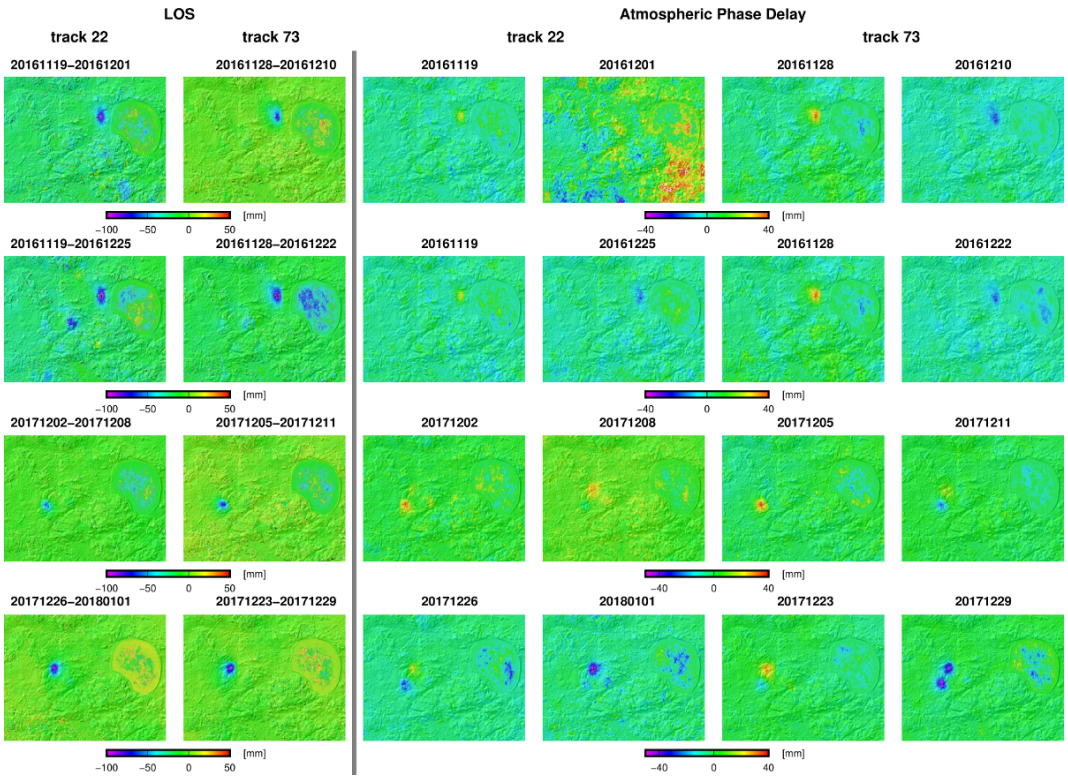

Fig. 32: Displacement results for three selected mining tremors. Left-hand side: displacement results for the two paths. Right-hand side: results of atmospheric components before and after the tremor, respectively (**O1**).

method should not be applied in areas where ground surface deformations are not time-constant. The method may be used, however, in such regions as the LGCB, where the employed mining system results in relatively time-constant displacements. The results indicate that the method is effective at detecting changes resulting from induced seismic events. It allows determining tremor locations in cases when acquisition dates are greater than the optimal value of 6-12 days (in the case of Sentinel 1A/B).

Summary

Classical geodetic surveys remain the most important source of data in mining areas and serve to identify the influence of mining exploitation on the ground surface. Surface displacements in mining areas are still one of the most important negative results of human intervention in the rock mass. State of the art knowledge regarding synthetic aperture radar interferometry, as well as the available data and calculation methods allow this approach to be used as an additional and independent source of information on surface displacement. I believe that the scientific achievement presented in this summary constitutes an important contribution to the research on applying satellite radar data to determine the influence of mining activity on the ground surface.

I also believe that I achieved the goal of my single-theme publication series. The most important conclusions from my research, as presented in publications (**O1** – **O8**), are provided below. The conclusions are grouped with respect to the particular research goals presented at the beginning of this summary.

With regard to demonstrating the possibility of applying the time-series type InSAR methods (PSInSAR and SBAS) to investigate long-term surface displacements in mining and post-mining areas,

- I demonstrated the possibility to conduct long-term (15 years) historical analyses of displacements in mining and post-mining areas on the basis of the PSInSAR method and data obtained from the ERS1/2 and Envisat satellites.
- I demonstrated the possibility to simultaneously analyze SAR data from different satellites.
- I used archive SAR data to demonstrate a direct correlation between rising underground water levels and upward movements of post-mining grounds.
- I also demonstrated that in the case of post-mining areas in Walbrzych, the influence of water table level reconstruction was observed directly above the reservoir.
- My calculation results allowed time-tracing the changes in the post-mining Walbrzych region. I precisely defined the regions in which terrain uplifts and subsidences were observed during the post-mining period.
- Based on the analysis of characteristic points located within the area of all water reservoirs, I demonstrated that the initial period of surface uplift is followed by a short period of stagnation. The uplift period is directly related to the restoration of groundwater table level. After the stagnation period, a sort of displacement adjustment may be observed. This adjustment is characterized by ground subsidence and followed by eventual surface stabilization.
- With respect to publication (**O7**), I demonstrated that synthetic aperture radar interferometry may be successfully employed in the detection of displacements in an open cast mine. I also demonstrated that without allowance for corrections due to the signal passing through the ionosphere and the troposphere, InSAR calculation methods may serve only as a complementary source of information.
- I demonstrated that with a large SAR data base and with the SBAS method, it is possible to trace the dynamics of the influence of underground copper ore mining on the surface (**O1**).

Additionally, publication (**O6**), which discusses the use of SAR data in the analysis of displacements during the post-mining period in relation to the whole closed hard coal basin, is the first of this type in Poland. Article (**O7**) is the first in Poland and one of the first in the world to discuss the application of SAR data from satellite Sentinel 1A/B and the SBAS method to evaluate surface activity in an open cast mine.

With regard to developing a method for simultaneous estimation of the influence of tropospheric and ionospheric delay on the calculated SAR data,

- I developed a method for simultaneous estimation of atmospheric delays in DInSAR calculations, which I successfully used, among others in the area of underground copper ore mining. The method is based on the use of the following models:

  - Generic Atmospheric Correction Online Service for InSAR (GACOS) - for calculating tropospheric delay,
  - Split-Spectrum - for calculating ionospheric delay.

- I demonstrated that my implementation of atmospheric delay estimation method does not affect the maximum values of surface displacements.

- Based on calculations performed for the regions of LGCB (mining tremors) and Chile (natural earthquakes), I concluded that by applying the method of my proposal it is possible to significantly reduce local displacement variations and also to significantly improve the general results.

With regard to demonstrating the possibility of applying InSAR methods in the detection of induced seismic events in mining areas,

- I demonstrated the possibility to use data provided by the Sentinel 1A/B satellites to detect surface changes due to mining tremors.

- In order to more precisely analyze the impact of a mining tremor on the ground surface, I proposed calculations employing two independent methods: DInSAR and SBAS.

- I conducted a series of test calculations based on the Mogi model, which was developed to test ground deformations in the vicinity of volcanoes. The purpose of these test calculations was to investigate the influence of the allowance for the empirical model for the elimination of atmospheric delay on SAR data calculations performed with the SBAS method.

- I demonstrated that including the empirical atmospheric delay estimation model (Tymofyeyeva and Fialko, 2015) allows the detection of the influence of a mining tremor on the surface.

- Based on the analysis of 23 mining tremors from the LGCB region (between 2014 and 2018), I demonstrated that tremor detection based on SAR data obtained over a period greater than 6 – 12 days is difficult due to the influence of mining activity observed in the signal phase. I also demonstrated that in such cases, the model (Tymofyeyeva and Fialko, 2015) allows precise separation of two interferogram phase components: the component due to the tremor from the displacement due to mining activity.

5. **Description of other scientific achievements**

The rest of my scientific research, apart from the above described achievement, focused mainly on the research areas presented below.

Surface displacement measurements in post-mining areas with the use of classical measurement methods and evaluation of the influence of ceased mining activity on the ground surface.

During my doctoral studies, I conducted geodetic surveys in the post-mining area of Walbrzych. As part of research grant no. N524 465436 (*Analysis of Changes on the Surface of Post-Mining Rock Mass in a Selected Region of the Former Walbrzych Basin*), I proposed and designed a measurement network, and subsequently I used it to perform precise leveling and GNSS measurements. The purpose of the research work was to evaluate the geometric condition of the rock mass surface in a selected part of the former Walbrzych Hard Coal Basin during coal production and after mining activity ceased.

Between 2014 and 2017 I was the head of a research project financed by the National Fund for Environmental Protection and Water Management. The project was carried out by Wroclaw University of Science and Technology on the order of the city of Walbrzych. The purpose of the project titled *Evaluation of Ground Surface Activity in the Post-Mining Area of the Former Walbrzych Coal Mines* was among others to analyze, design and increase the density of lower precision survey lines, as well as performing 4 measurement campaigns. As part of the first stage, I prepared an inventory of the already existing elevation points in the area of Walbrzych and its surroundings. The results served me to prepare a design of a control survey comprising second- and third-class points, as well as points of the mine networks. The total number of survey points in the network was 487, and the total length of the level circuit sections was 86 km. Additionally, in the regions in which the existing point network was insufficient, I installed extra benchmarks – a total of 24. Four measurement campaigns (precise leveling) were performed on the network thus prepared. They were conducted between November 2014 and May 2016.

Of the 487 analyzed benchmark points, 78 showed significant displacements. Over the analyzed time, the Old Town region subsided by approximately -6.5 mm. Maximum vertical displacements (between November 2014 and November 2015) were observed on benchmarks 1077 and 1076 (area of the Glowackiego St.) – they exceeded -10.5 mm. The greatest number of "active" benchmark points was located in the Old Town area, as well as along the 11-Listopada Street. Displacements were also observed in the regions of 1-Maja and Piasta streets.

I also analyzed ground surface changes in the area of the closed "Konrad" mine in Iwiny (Głowacki and Milczarek, 2013).

My research works at that time resulted in the following publications and reports:

- Blachowski J., **Milczarek W.**, Analysis of surface changes in the Wałbrzych hard coal mining grounds (SW Poland) between 1886 and 2009. Geological Quarterly. 2014, vol. 58, nr 2, s. 353-367
  IF = 1.000, **20 MoSaHE (MNiSW) points**
- Blachowski J., **Milczarek W.**, Stefaniak P.,Deformation information system for facilitating studies of mining-ground deformations, development, and applications. Natural Hazards and Earth System Sciences. 2014, vol. 14, nr 7, s. 1677-1689
- Blachowski J., **Milczarek W.**, Deformacje wtórne terenów górniczych na obszarze dawnego Zagłębia Wałbrzyskiego. W: Miernictwo górnicze i ochrona terenów górniczych w obecnych warunkach wydobycia surowców mineralnych w Polsce, Wydawnictwa AGH, Kraków, 2016 113-123.
- **Milczarek W.**, Blachowski J., Wałbrzyskie Zagłębie Węglowe – aktualny stan wiedzy na temat pogórniczych deformacji powierzchni terenu. W: (red. Przylibski T.) Mat. III Polski Kongres Górniczy 2015, Wrocław, s. 486-488.

- Cacoń S., Blachowski J., **Milczarek W.**, Problem układu odniesienia dla sieci geodezyjnej w monitorowaniu deformacji terenów górniczych. Przegląd Górniczy, 2013, 8, 14-19.
- Głowacki T., **Milczarek W.**, Surface deformation of the secondary former mining areas. W: 11. Altbergbau-Kolloquium und 7. Konferenz Erbe und Geschichte des Bergbaus : 700 Jahre Kupfererzbergbau in Niederschlesien, 03. bis 05. November 2011, Wrocław / [Hrsg. G. Meier i in.]. Essen : VGE Verlag GmbH, cop. 2011. s. 182-197.

Ground-based laser scanning for measuring the deformations of engineering structures and for documenting old workings

During the first years after being awarded doctoral degree, I conducted research into the application of ground-based laser scanning in measuring deformations of engineering structures (cooling towers, smokestacks), making inventory of old workings in mines and of architectural objects. My research works at that time resulted in the following publications and reports:

- Kądzioła K., Kasza D., **Milczarek W.**, Three-dimensional model of the Rzeczka object (the Riese Complex, Sowie Range) as an enhancement of the comprehensive geotourism potential of an underground tourist route, XXIIIrd Autumn School of Geodesy, Wałbrzych, Poland, September 21-22, 2017 / Jan B. Blachowski, J. Górniak-Zimroz and D. Kasza (Eds.),EDP Sciences, 2018. art. 00015, s. 1-8., (E3S Web of Conferences, ISSN 2267-1242; vol. 55),
- Muszyński Z., **Milczarek W.**, Application of terrestrial laser scanning to study the geometry of slender objects, World Multidisciplinary Earth Sciences Symposium: 11-15 September 2017, Prague, Czech Republic, IOP Publishing, 2017. art. 042069, s. 1-7. (IOP Conference Series - Earth and Environmental Science, ISSN 1755-1315; vol. 95)
- Wajs J., **Milczarek W.**, Głowacki T., Pomiary geometrii hiperboidalnych chłodni kominowych metodą naziemnego skaningu laserowego. W: Zagadnienia interdyscyplinarne w górnictwie i geologii: XVI Konferencja Doktorantów i Młodych Uczonych, Szklarska Poręba, 17-20 maja 2016
- Kasza D., **Milczarek W.**, Wajs J., Modelowanie 3D obiektów podziemnych z chmury punktów na przykładzie Jaskini Niedźwiedziej w Kletnie. Zagadnienia interdyscyplinarne w górnictwie i geologii: XVI Konferencja Doktorantów i Młodych Uczonych, Szklarska Poręba, 17-20 maja 2016
- Kasza D., **Milczarek W.**, Modelowanie obiektów podziemnych oraz struktur geologiczno-tektonicznych z chmury punktów, XV Konferencja Doktorantów i Młodych Uczonych, Szklarska Poręba, 20-22 maja 2015
- Muszyński Z., **Milczarek W.**, Modelowanie przemieszczeń pionowych na podstawie danych z naziemnego skanera laserowego. Geoinformacja jako metoda ochrony przed geozagrożeniami / pod red. Krzysztofa Karszni i Konrada Podawcy. Warszawa, Wydawnictwo SGGW, 2014. s. 42-63.
- Muszyński Z., Głowacki T., **Milczarek W.**, Wajs J., Słoniński T., Grygiel A., Geodezja pomiary przemieszczeń i odkształceń chłodni kominowej W-2/2 w Elektrowni Bełchatów wraz z opracowaniem wyników. Raporty Wydziału Geoinżynierii, Górnictwa i Geologii Politechniki Wrocławskiej. 2016, Ser. SPR nr 14, 111 s
- Muszyński Z., Głowacki T., **Milczarek W.**, Wajs J., Słoniński T., Grygiel A., Badania specjalistyczne stanu geometrycznego chłodni hiperboloidalnych huty miedzi Głogów I i II. Raporty Wydziału Geoinżynierii, Górnictwa i Geologii Politechniki Wrocławskiej. 2015, Ser. SPR nr 20, 48 s.
- Głowacki T., Dudek A., Muszyński Z., **Milczarek W.**, Wajs J., Kasza D., Grygiel A., Badania specjalistyczne stanu geometrycznego chłodni hiperboloidalnych huty miedzi Głogów I i II. Raporty Inst. Gór. PWroc. 2014, Ser. SPR nr 3, 92 s.
- Głowacki T., Dudek A., Muszyński Z., **Milczarek W.**, Wajs J., Grygiel A., Badania specjalistyczne stanu geometrycznego chłodni hiperboloidalnych huty miedzi Głogów I i II. Raporty Inst. Gór. PWroc. 2014, Ser. SPR nr 24, 60 s.

- Głowacki T., **Milczarek W.**, Dudek A., Śliwonik W., Grygiel A., Operat geodezyjny : aktualizacja oraz poszerzenie obszaru objętego mapami dla wybranych terenów pogórniczych "Kopalni Św. Jana" w Krobicy. Raporty Inst. Gór. PWroc. 2011, Ser. SPR nr 10, 7 s.

As the supervisor of a students' research group named "Young Geodesists Group", I initiated works related to the use of ground-based laser scanning in determining avalanche risk in selected parts of the Sudety Mountains. These works resulted in laser scanning measurements of selected regions in the Sudety Mountains (Bialy Jar, Kociol Lomniczki, Kociol Malego Stawu and Kociol Wielkiego Stawu).

The result of my work was also the following diploma theses carried out under my supervision:

- *Development of measurements of cooling tower made using terrestrial laser scanning*, BSc Thesis (work awarded), Diana Piróg, 2014,
- *Measurement of telecommunications mast tilting by a tacheometric method and laser scanning*, BSc Thesis , Michał Najdek, 2014,
- *Assessment of accuracy of measurement using terrestrial laser scanning depending on the scanned surface*, BSc Thesis , Karolina Karwowska, 2014,
- *Development of a spatial model of Aula Leopoldin using laser scanning*, master thesis (work awarded), Barbara Kubiak, 2016,

Application of Geographic Information System in the analyses of the influence of mining activity on the ground surface

Part of my scientific activity is related to the broadly understood Geographic Information Systems (GIS). Already since my PhD program and until today, I have used GIS tools to collect and process data as well as to analyze the obtained results. As a PhD student and in the first years after obtaining the doctoral degree, I used GIS tools to collect spatial data related to: mining operations in the Walbrzych area, as well as geological and survey data. Based on the geological data obtained from Polish Geological Institute, I designed a spatial geological model which served me to prepare geometric models used in my further numerical calculations. I currently use GIS tools to analyze the results of radar data calculations – especially the PSInSAR and SBAS data. My research works at that time resulted in the following publications and reports:

- Blachowski J., Górniak-Zimroz J., **Milczarek W.**, Pactwa K., Applications of geomatics in surface mining, World Multidisciplinary Earth Sciences Symposium: 11-15 September 2017, Prague, Czech Republic,IOP Publishing, 2017. art. 042009, s. 1-9, (IOP Conference Series - Earth and Environmental Science, ISSN 1755-1315; vol. 95)
- **Milczarek W.**, Określenie aktywności powierzchni górotworu po zakończonej eksploatacji na obszarze byłych kopalń wałbrzyskich. Raporty Wydziału Geoinżynierii, Górnictwa i Geologii Politechniki Wrocławskiej. 2017, Ser. SPR nr 2, 580 s.
- Blachowski J., Grzempowski P., **Milczarek W.**, Nowacka A., Opracowanie metody numerycznego modelowania deformacji terenu górniczego w złożonych geologiczno-górniczych warunkach eksploatacji. Raporty Wydziału Geoinżynierii, Górnictwa i Geologii Politechniki Wrocławskiej. 2016, Ser. SPR nr 7, 15, [2] s.
- Blachowski J., **Milczarek W.**, Woźniak J., Opracowanie punktowej mapy geologiczno-inżynierskiej w ramach realizacji zadań z zakresu wspomagania systemów gromadzenia i przetwarzania danych związanych z dostępem do informacji o środowisku dla Wydziału Ochrony Środowiska i Rolnictwa Urzędu Miasta Opole. Raporty Inst. Gór. PWroc. 2011, Ser. SPR nr 45, 12 s.
- Blachowski J., **Milczarek W.**, 2011, Development and application of 3D geological model and geoinformation system for numerical modelling of ground deformations in abandoned underground coal mines. W: Mathematical geosciences at the crossroads of theory and practice, Proceedings of the IAMG 2011 Conference, September 5-9, 2011, Salzburg, Austria, (Red) Robert Marschallinger, Fritz Zobl, ÖAW. Austrian Academy of Sciences. s. 837-851,

Application of numerical modeling (finite element method) in evaluating the influence of underground mining on the ground surface

During the first years after obtaining the doctoral degree, I continued my research related to the application of finite element method in evaluating the influence of underground mining on the ground surface. In 2012, I was appointed as a visiting researcher for three months at the University of New Brunswick (Canada), during which I continued the research works I had started during my doctoral program – application of numerical modeling in the evaluation of the influence of underground mining on the ground surface. My research work at that time resulted in the following publication:

- Chrzanowska A., **Milczarek W.**, Bazanowski M., Wyznaczanie rozkładu naprężeń i deformacji w naruszonym górotworze. Ochrona obiektów na terenach górniczych, praca zbiorowa / pod red. Andrzeja Kowalskiego. Katowice: GIG, 2012. s. 254-264.

Signature of the applicant

Literatura

Antonello G., Casagli N., Farina P., Leva D., Nico G., Sieber A.J., Tarchi D. Ground-based SAR interferometry for monitoring mass movements. *Landslides*, 1(1):21–28, 2004. ISSN 1612-5118. doi:10.1007/s10346-003-0009-6.

Barnhart W.D., Benz H.M., Hayes G.P., Rubinstein J.L., Bergman E., Benz H.M., Hayes G.P., Rubinstein J.L., Bergman E. Journal of Geophysical Research : Solid Earth. *Journal of Geophysical Research : Solid Earth*, (Figure 1):1–11, 2014. doi:10.1002/2014JB011227.Received.

Bekaert D.P.S., Walters R.J., Wright T.J., Hooper A.J., Parker D.J. Statistical comparison of InSAR tropospheric correction techniques. *Remote Sensing of Environment*, 170:40–47, 2015. ISSN 0034-4257. doi: 10.1016/j.rse.2015.08.035.

Bischoff M., Cete A., Fritschen R., Meier T. Coal mining induced seismicity in the Ruhr area, Germany. *Pure and Applied Geophysics*, 167(1-2):63–75, 2010. ISSN 00334553. doi:10.1007/s00024-009-0001-8.

Blachowski J., Kopeć A., Milczarek W., Owczarz K. Evolution of secondary deformations captured by satellite radar interferometry: Case study of an abandoned coal basin in sw poland. *Sustainability*, 11(3), 2019. ISSN 2071-1050.

Brcic R., Parizzi A., Eineder M., Bamler R., Meyer F. Estimation and compensation of ionospheric delay for SAR interferometry. *International Geoscience and Remote Sensing Symposium (IGARSS)*, (3):2908–2911, 2010. ISSN 2153-6996. doi:10.1109/IGARSS.2010.5652231.

Bürgmann R., Rosen P.A., Fielding E.J. Synthetic Aperture Radar Interferometry to Measure Earth's Surface Topography and Its Deformation. *Annual Review of Earth and Planetary Sciences*, 28(1):169–209, 2000. doi: 10.1146/annurev.earth.28.1.169.

Carlà T., Farina P., Intrieri E., Ketizmen H., Casagli N. Integration of ground-based radar and satellite InSAR data for the analysis of an unexpected slope failure in an open-pit mine. *Engineering Geology*, 235(December 2017):39–52, 2018. ISSN 00137952. doi:10.1016/j.enggeo.2018.01.021.

Chaussard E., Bürgmann R., Shirzaei M., Fielding E.J., Baker B. Journal of Geophysical Research : Solid Earth. *Journal of Geophysical Research : Solid Earth*, 1–19, 2014. ISSN 21699313. doi: 10.1002/2014JB011266.Received.

Cuenca C.M., Hooper A.J., Hanssen R.F. Surface deformation induced by water influx in the abandoned coal mines in Limburg, The Netherlands observed by satellite radar interferometry. *Journal of Applied Geophysics*, 88:1–11, 2013. ISSN 09269851. doi:10.1016/j.jappgeo.2012.10.003.

Doin M.P., Lasserre C., Peltzer G., Cavalié O., Doubre C. Corrections of stratified tropospheric delays in SAR interferometry: Validation with global atmospheric models. *Journal of Applied Geophysics*, 69(1):35–50, 2009. ISSN 0926-9851. doi:10.1016/j.jappgeo.2009.03.010.

Doležalová H., Kajzar V., Souček K., Staš L. Evaluation of mining subsidence using GPS data. *Acta Geodynamica et Geomaterialia*, 6(3):359–367, 2009. ISSN 12149705.

Drzewiecki J., Piernikarczyk A. The forecast of mining-induced seismicity and the consequent risk of damage to the excavation in the area of seismic event. *Journal of Sustainable Mining*, 16(1):1–7, 2017. ISSN 23003960. doi:10.1016/j.jsm.2017.05.001.

Duque S., Lopez-Sanchez J., Mallorqui J., Herrera G., Tomás R., Mulas J., Delgado J. Advanced DInSAR analysis on mining areas: La Union case study (Murcia, SE Spain). *Engineering Geology*, 90(3-4):148–159, 2007. ISSN 00137952. doi:10.1016/j.enggeo.2007.01.001.

Fattahi H., Simons M., Agram P. InSAR Time-Series Estimation of the Ionospheric Phase Delay: An Extension of the Split Range-Spectrum Technique. *IEEE Transactions on Geoscience and Remote Sensing*, 55(10):5984–5996, 2017. ISSN 01962892. doi:10.1109/TGRS.2017.2718566.

Gee D., Bateson L., Sowter A., Grebby S., Novellino A., Cigna F., Marsh S., Banton C., Wyatt L. Ground Motion in Areas of Abandoned Mining: Application of the Intermittent SBAS (ISBAS) to the Northumberland and Durham Coalfield, UK. *Geosciences*, 7(3):85, 2017. ISSN 2076-3263. doi:10.3390/geosciences7030085.

Gibowicz S., Kijko A. *An Introduction to Mining Seismology*. Academic Press, 1994.

Gomba G., Parizzi A., Zan F.D., Eineder M., Member S., Bamler R. New_electric_propulsion.pdf. 54(3):1446–1461, 2016. ISSN 0196-2892. doi:10.1109/TGRS.2015.2481079.

González P.J., Bagnardi M., Hooper A.J., Larsen Y., Marinkovic P., Samsonov S.V., Wright T.J. The 2014-2015 eruption of Fogo volcano: Geodetic modeling of Sentinel-1 TOPS interferometry. *Geophysical Research Letters*, 42(21):9239–9246, 2015. ISSN 19448007. doi:10.1002/2015GL066003.

Głowacki T., Milczarek W. Surface deformation of the secondary former mining areas. *Mining Science*, 20:39–55, 2013. ISSN 2300-9586. doi:10.5277/gig132004.

Henderson S.T., Pritchard M.E. Decadal volcanic deformation in the central andes volcanic zone revealed by InSAR time series. *Geochemistry, Geophysics, Geosystems*, 14(5):1358–1374, 2013. ISSN 15252027. doi:10.1002/ggge.20074.

Hussain E., Hooper A., Wright T.J., Walters R.J., Bekaert D.P. Interseismic strain accumulation across the central North Anatolian Fault from iteratively unwrapped InSAR measurements. *Journal of Geophysical Research: Solid Earth*, 121(12):9000–9019, 2016. ISSN 21699356. doi:10.1002/2016JB013108.

Jung H.C., Kim S.W., Jung H.S., Min K.D., Won J.S. Satellite observation of coal mining subsidence by persistent scatterer analysis. *Engineering Geology*, 92(1):1–13, 2007. ISSN 0013-7952. doi:https://doi.org/10.1016/j.enggeo.2007.02.007.

Kubacki T., D. K.K., L. P.K., K. M.M. Changes in mining-induced seismicity before and after the 2007 Crandall Canyon Mine collapse. *Journal of Geophysical Research: Solid Earth*, 119(6):4876–4889, ???? doi:10.1002/2014JB011037.

Kusznir N.J., Ashwin D.P., Bradley A.G. Mining induced seismicity in the North Staffordshire coalfield, England. *International Journal of Rock Mechanics and Mining Sciences & Geomechanics Abstracts*, 17(1):45–55, 1980. ISSN 0148-9062. doi:https://doi.org/10.1016/0148-9062(80)90005-4.

Li Z., Fielding E.J., Cross P., Preusker R. Advanced InSAR atmospheric correction: MERIS/MODIS combination and stacked water vapour models. *International Journal of Remote Sensing*, 30(13):3343–3363, 2009. ISSN 0143-1161. doi:10.1080/01431160802562172.

Liu D., Shao Y., Liu Z., Riedel B., Sowter A., Niemeier W., Bian Z. Evaluation of InSAR and TomoSAR for Monitoring Deformations Caused by Mining in a Mountainous Area with High Resolution Satellite-Based SAR. *Remote Sensing*, 6(2):1476–1495, 2014. ISSN 2072-4292. doi:10.3390/rs6021476.

Ma C., Cheng X., Yang Y., Zhang X., Guo Z., Zou Y. Investigation on Mining Subsidence Based on Multi-Temporal InSAR and Time-Series Analysis of the Small Baseline Subset—Case Study of Working Faces 22201-1/2 in Bu'ertai Mine, Shendong Coalfield, China. *Remote Sensing*, 8(11), 2016. ISSN 2072-4292. doi:10.3390/rs8110951.

Malinowska A.A., Witkowski W.T., Guzy A., Hejmanowski R. Mapping ground movements caused by mining-induced earthquakes applying satellite radar interferometry. *Engineering Geology*, 246(August):402–411, 2018. ISSN 00137952. doi:10.1016/j.enggeo.2018.10.013.

Milczarek W. Investigation of post inducted seismic deformation of the 2016 mw 4.2 tarnovek poland mining tremor based on dinsar and sbas method. *Acta Geodynamica et Geomaterialia*, 194(2):402–411, 2019. ISSN 1214-9705.

Paradella W.R., Ferretti A., Mura J.C., Colombo D., Gama F.F., Tamburini A., Santos A.R., Novali F., Galo M., Camargo P.O., Silva A.Q., Silva G.G., Silva A., Gomes L.L. Mapping surface deformation in open pit iron mines of Carajás Province (Amazon Region) using an integrated SAR analysis. *Engineering Geology*, 193:61–78, 2015. ISSN 0013-7952. doi:https://doi.org/10.1016/j.enggeo.2015.04.015.

Peduto D., Nicodemo G., Maccabiani J., Ferlisi S. Multi-scale analysis of settlement-induced building damage using damage surveys and DInSAR data: A case study in The Netherlands. *Engineering Geology*, 218:117–133, 2017. ISSN 00137952. doi:10.1016/j.enggeo.2016.12.018.

Remy D., Chen Y., Froger J.L., Bonvalot S., Cordoba L., Fustos J. Revised interpretation of recent InSAR signals observed at Llaima volcano (Chile). *Geophysical Research Letters*, 42(10):3870–3879, 2015. ISSN 19448007. doi:10.1002/2015GL063872.

Riemer K., Durrheim R. Mining seismicity in the Witwatersrand Basin: monitoring, mechanisms and mitigation strategies in perspective. *Journal of Rock Mechanics and Geotechnical Engineering*, 4(3):228–249, 2012. ISSN 16747755. doi:10.3724/SP.J.1235.2012.00228.

Rosen P.A., Hensley S., Chen C. Measurement and mitigation of the ionosphere in L-band Interferometric SAR data. *IEEE National Radar Conference - Proceedings*, 1459–1463, 2010. ISSN 10975659. doi:10.1109/RADAR.2010.5494385.

Samsonov S., Smets B., D'Oreye N., Smets B. Ground deformation associated with post-mining activity at the French – German border revealed by novel InSAR time series method. *International Journal of Applied Earth Observations and Geoinformation*, 23:142–154, 2013. ISSN 0303-2434. doi:10.1016/j.jag.2012.12.008.

Tong X., Sandwell D.T., Smith-Konter B. High-resolution interseismic velocity data along the San Andreas Fault from GPS and InSAR. *Journal of Geophysical Research: Solid Earth*, 118(1):369–389, 2013. ISSN 21699356. doi:10.1029/2012JB009442.

Tung S., Masterlark T. Coseismic slip distribution of the 2015 Mw7.8 Gorkha, Nepal, earthquake from joint inversion of GPS and InSAR data for slip within a 3-D heterogeneous Domain. *Journal of Geophysical Research: Solid Earth*, 121(5):3479–3503, 2016. ISSN 21699356. doi:10.1002/2015JB012497.

Tymofyeyeva E., Fialko Y. Mitigation of atmospheric phase delays in InSAR data, with application to the eastern California shear zone. *Journal of Geophysical Research: Solid Earth*, 120(8):5952–5963, 2015. ISSN 21699356. doi:10.1002/2015JB011886.

Wang W., Meng X., Peng Z., Chen Q.f., Liu N. Increasing background seismicity and dynamic triggering behaviors with nearby mining activities around Fangshan Pluton in Beijing, China. *Journal of Geophysical Research : Solid Earth*, 5624–5638, 2015. doi:10.1002/2015JB012235.Received.

Xu X., Sandwell D.T., Tymofyeyeva E., González-Ortega A., Tong X. Tectonic and Anthropogenic Deformation at the Cerro Prieto Geothermal Step-Over Revealed by Sentinel-1A InSAR. *IEEE Transactions on Geoscience and Remote Sensing*, 55(9):5284–5292, 2017. ISSN 0196-2892. doi:10.1109/TGRS.2017.2704593.

Yu C., Li Z., Penna N.T., Crippa P. Generic Atmospheric Correction Model for Interferometric Synthetic Aperture Radar Observations. *Journal of Geophysical Research: Solid Earth*, 9202–9222, 2018. ISSN 21699356. doi:10.1029/2017JB015305.

Yu C., Penna N.T., Li Z. Generation of real-time mode high-resolution water vapor fields from GPS observations. *Journal of Geophysical Research*, 122(3):2008–2025, 2017. ISSN 21562202. doi:10.1002/2016JD025753.

Zhao C., Lu Z., Zhang Q. Time-series deformation monitoring over mining regions with SAR intensity-based offset measurements. *Remote Sensing Letters*, 4(5):436–445, 2013. doi:10.1080/2150704X.2012.746482.

Zhu J., Chang Z., Li X., Yu J., Yu W., Luo Y., Wang W., Wan X., Qian S. An improved atmospheric correction method in repeat-pass InSAR measurements. *International Journal of Remote Sensing*, 39(21):7276–7292, 2018. ISSN 0143-1161. doi:10.1080/01431161.2018.1468112.